

DCH performance vs endcap shape and position

Matteo Rama
Giuseppe Finocchiaro
LNF
17 October 2012

Goals

- Evaluate the DCH performance as a function of the shape and position of the endcaps
 - p resolution
 - K/ π separation using dE/dx
 - B \rightarrow D* K reco. efficiency, ΔE
- All studies shown in these slides have been produced using FastSim V0.3.2

Five DCH configurations

common features:

- 10 superlayers, 4 layers each: A A S₊ S₋ S₊ S₋ S₊ S₋ A A
 - |stereo angle| ≈ 0.06 rad
 - inner wall radius: 26.5 cm
 - outer wall radius: 80.3 cm
 - sense wires r_{\min} : 28.6 cm
 - sense wires r_{\max} : 78.0 cm
- hit spatial resolution: babar-like
- hit efficiency vs polar angle: babar-like (babar-like: tuned on babar data)
- $\sigma(dE/dx)$ modelization: babar-like
 - $\sigma\left(\frac{dE}{dx}\right) = \alpha \left|\frac{dE}{dx}\right|^\beta dx^\gamma$ α, β, γ tuned on babar data

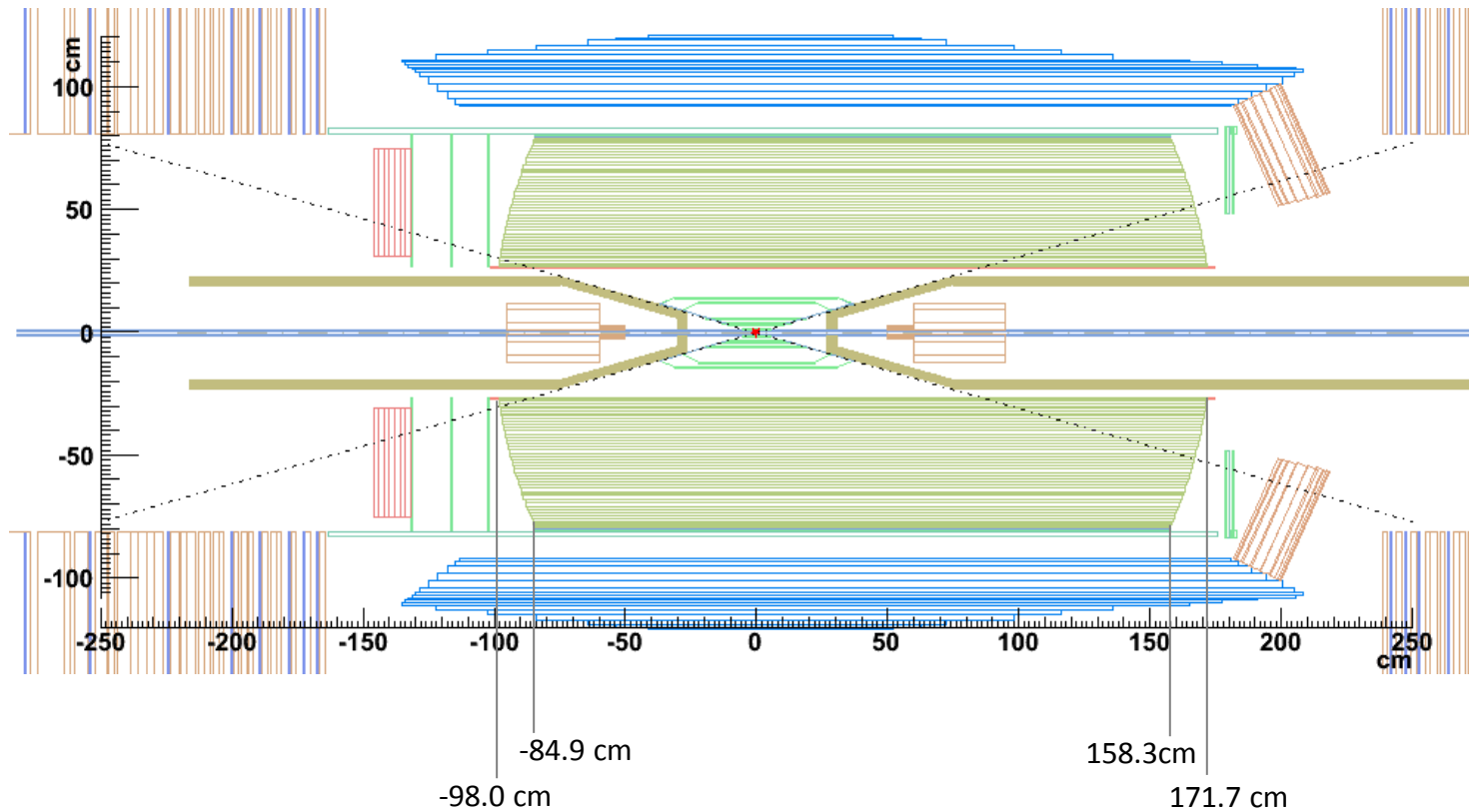
distinguishing features

- shape and position of endcaps
 - concave/convex
 - varying position along z

FastSim configurations based on drawings provided by S. Lauciani (see backup slides)

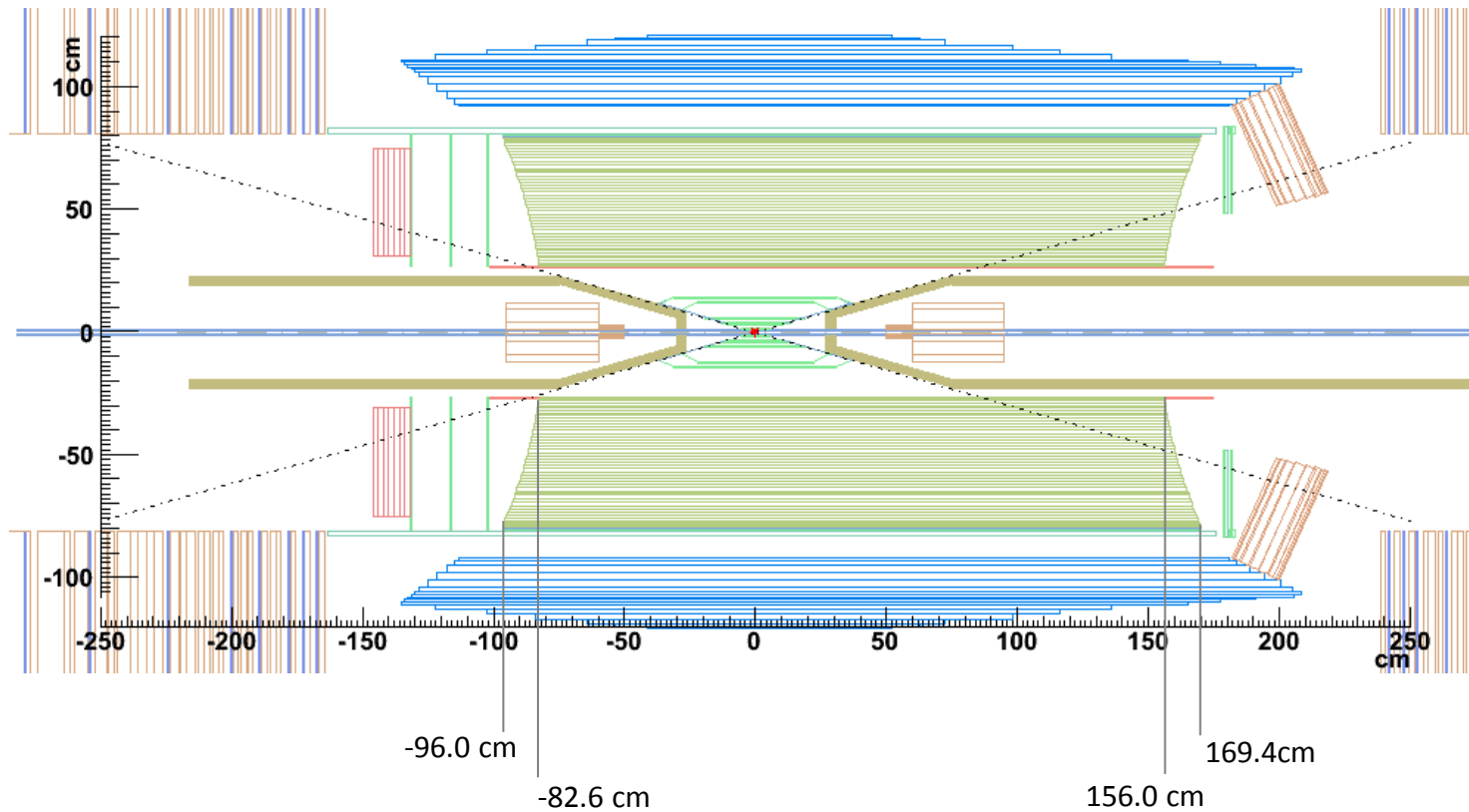
Option 1

x-z layout in fastsim



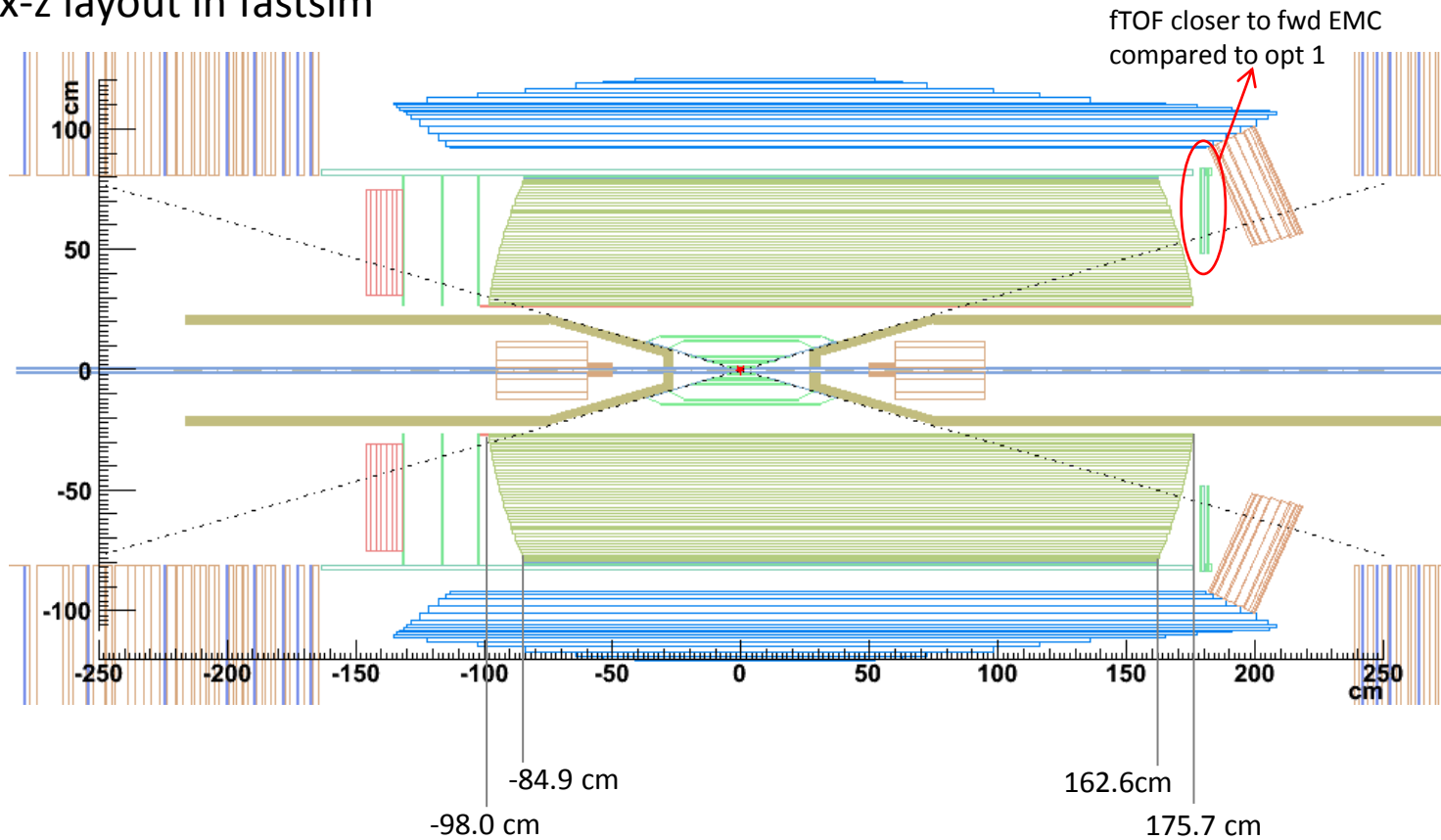
Option 2

x-z layout in fastsim



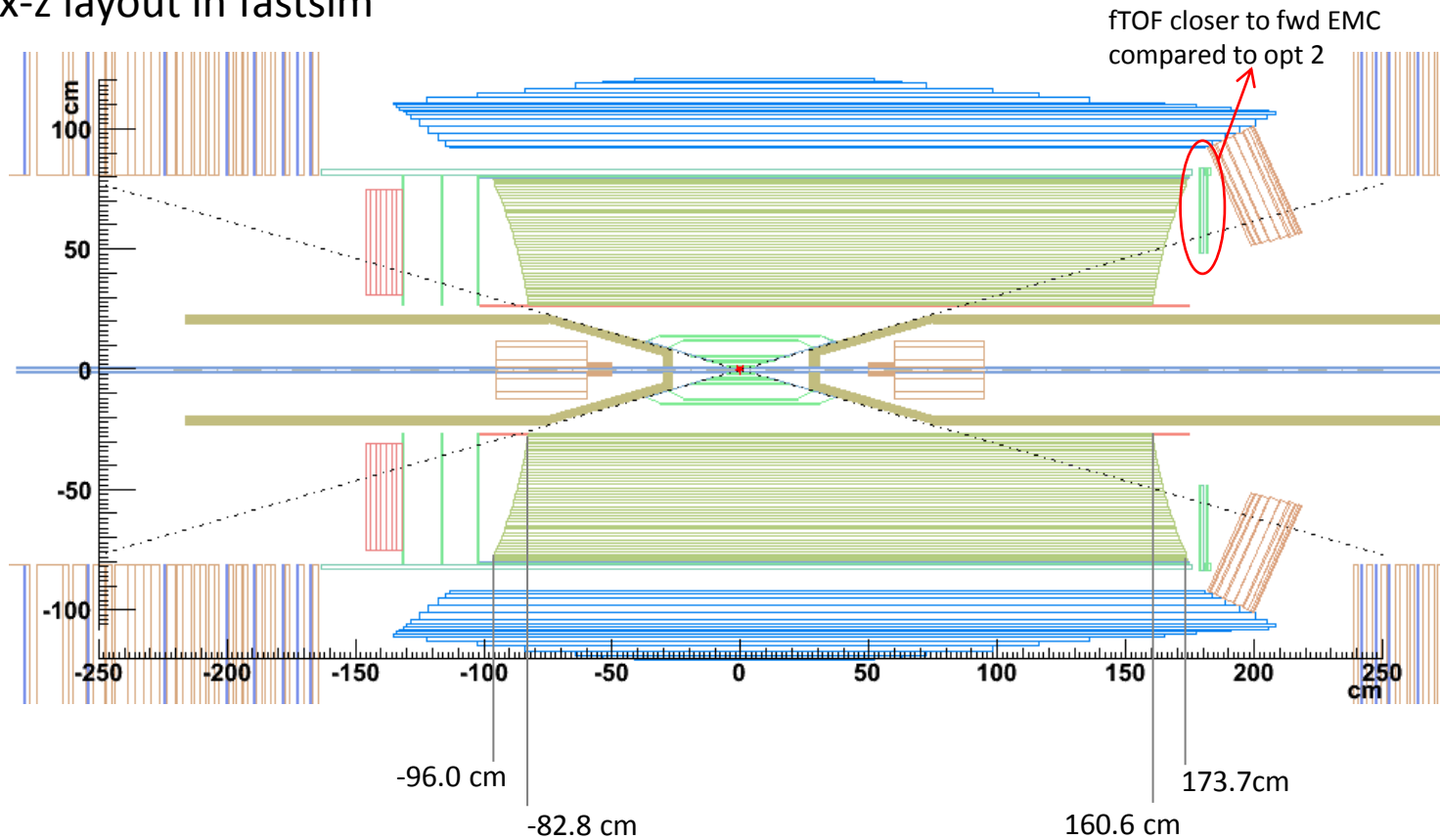
Option 3

x-z layout in fastsim



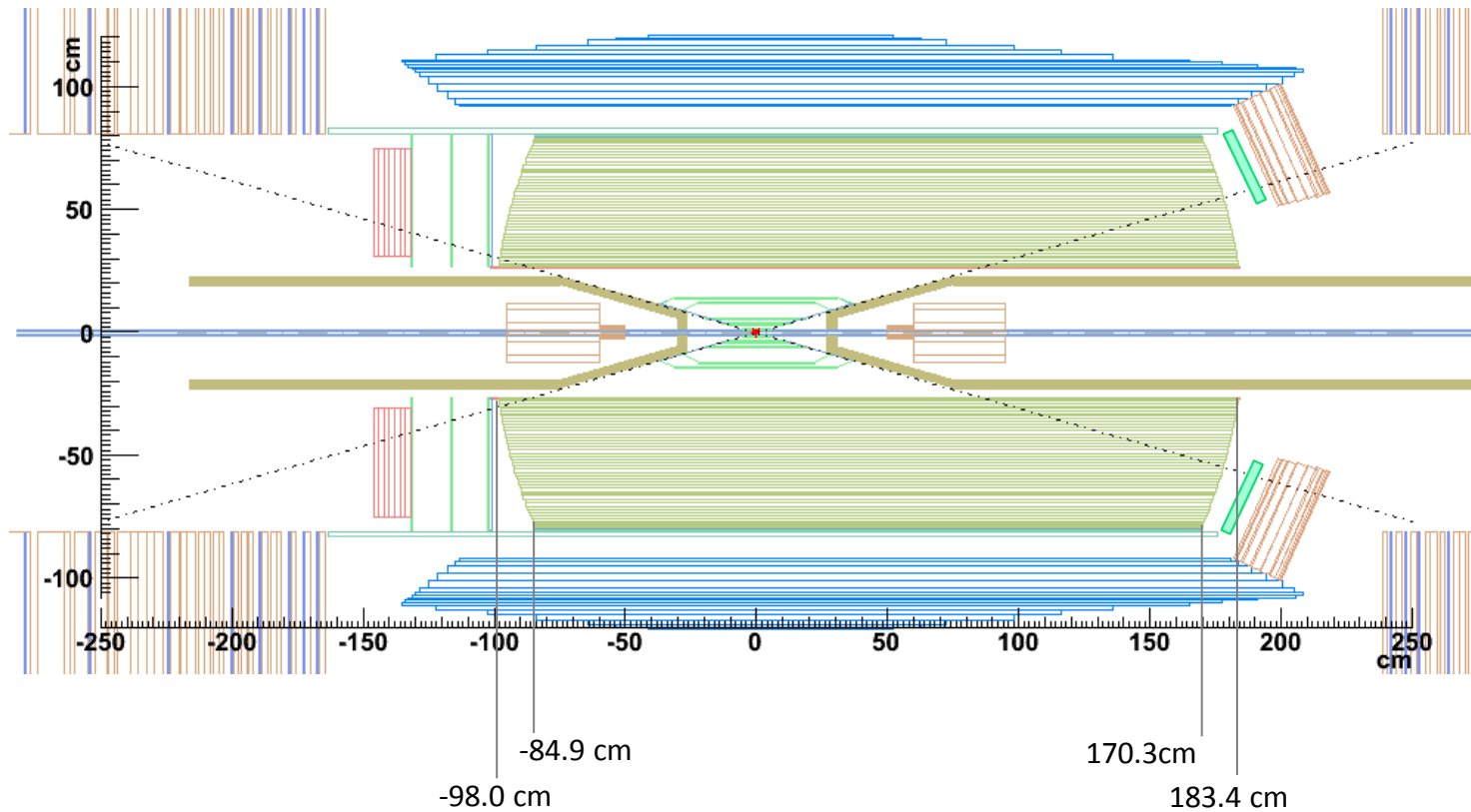
Option 4

x-z layout in fastsim



Option 5

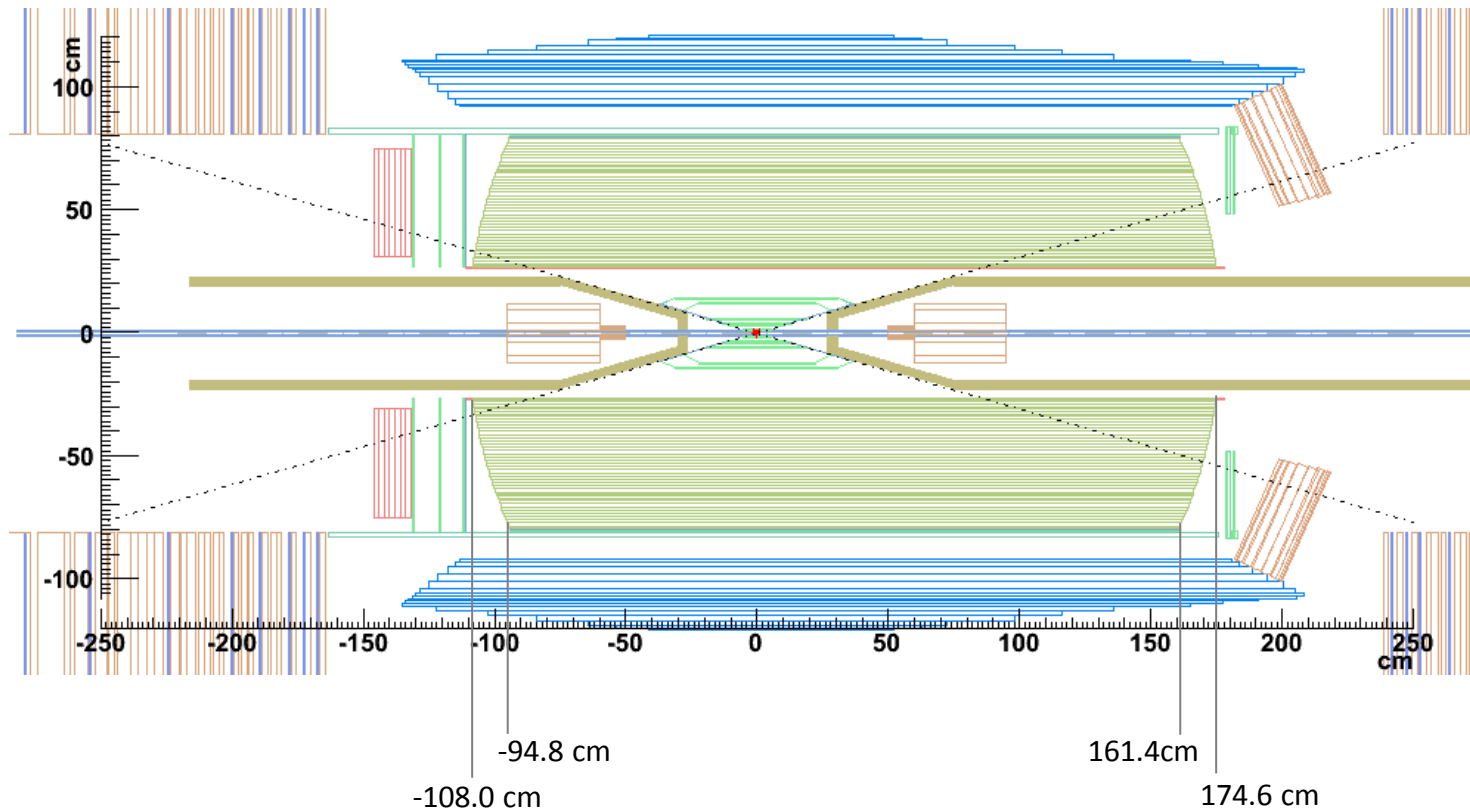
x-z layout in fastsim



Option 7

Note: Option 6 is a “babar-like” configuration. See backup slides.

x-z layout in fastsim



compared to Option 3:

1.1 cm shorter in forward direction, 10 cm longer in backward direction

Part I

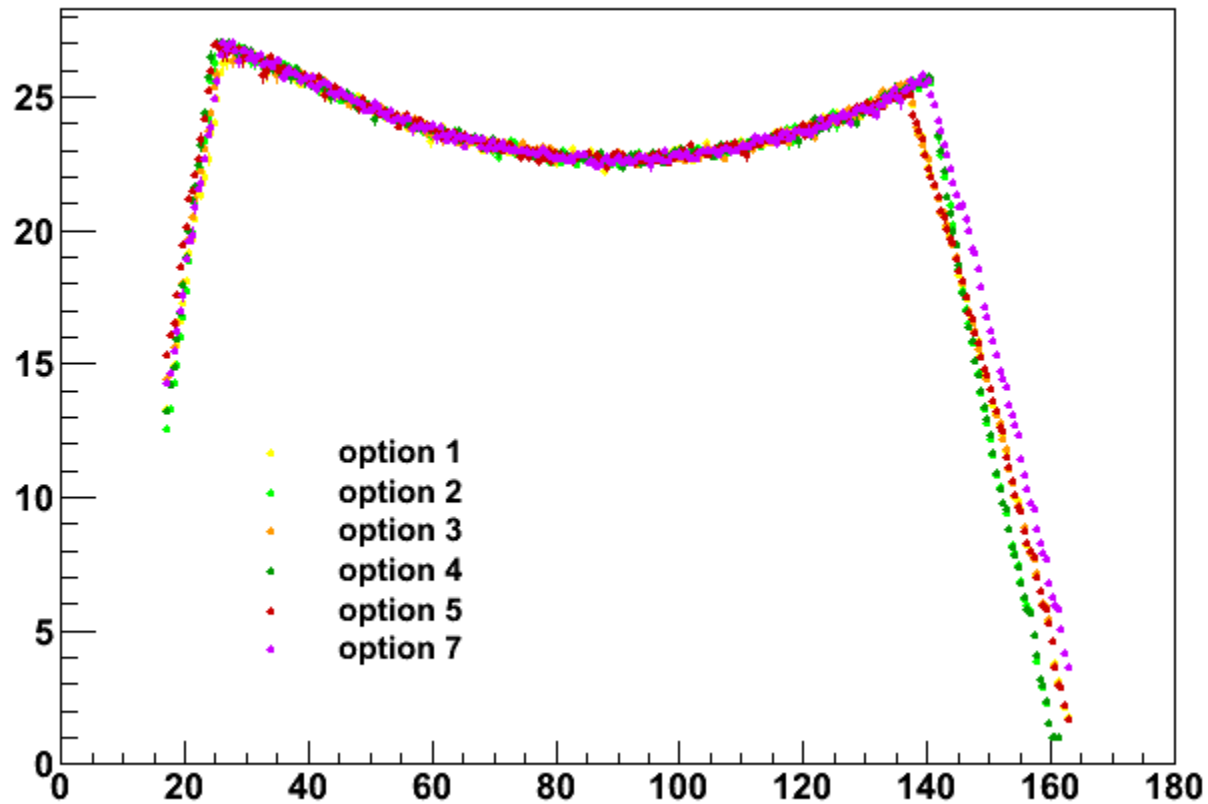
validation with $p = 4 \text{ GeV}/c$ single particles

single particles generated with:

- $p = 4 \text{ GeV}/c$
- $dP/ d\cos\theta = \text{const}$ [$\theta = \text{polar angle}$]
- $\cos\theta$ in $[0.3, \pi-0.3]$ rad [SVT angular acceptance]
- 50k events for each configuration

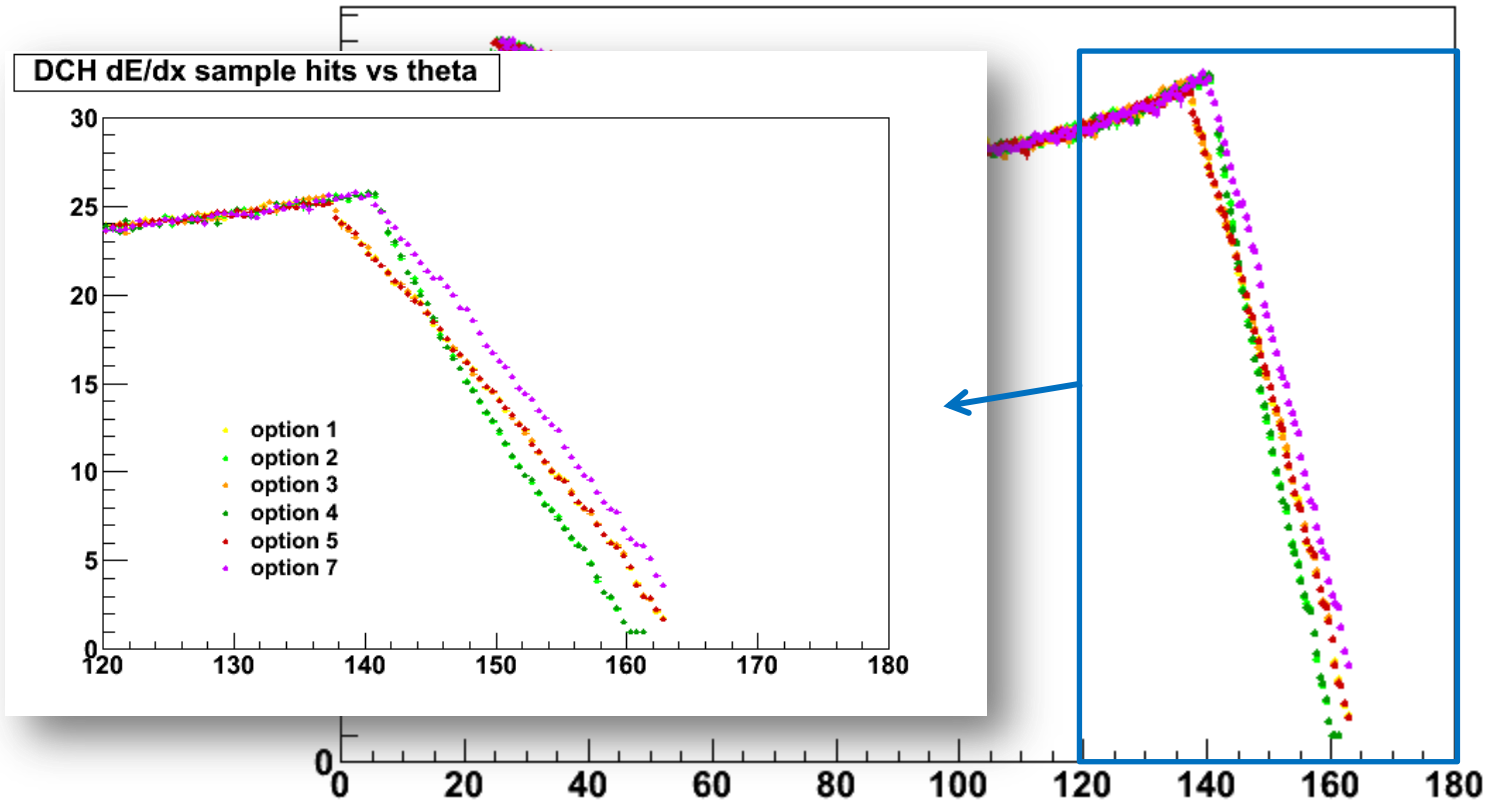
single π^+ , $p = 4\text{GeV}/c$, flat $\cos\theta$

DCH dE/dx sample hits vs theta



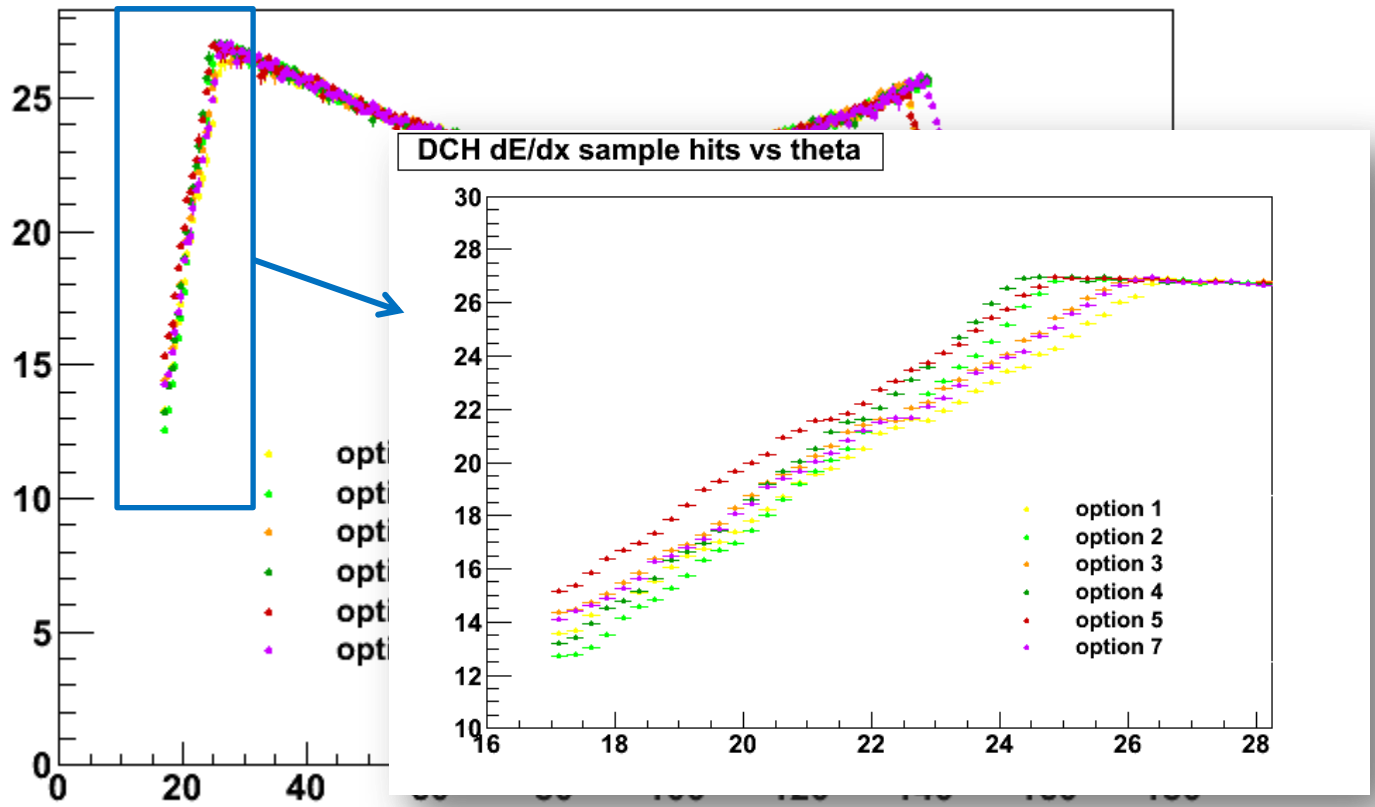
single π^+ , $p = 4\text{GeV}/c$, flat $\cos\theta$

DCH dE/dx sample hits vs theta

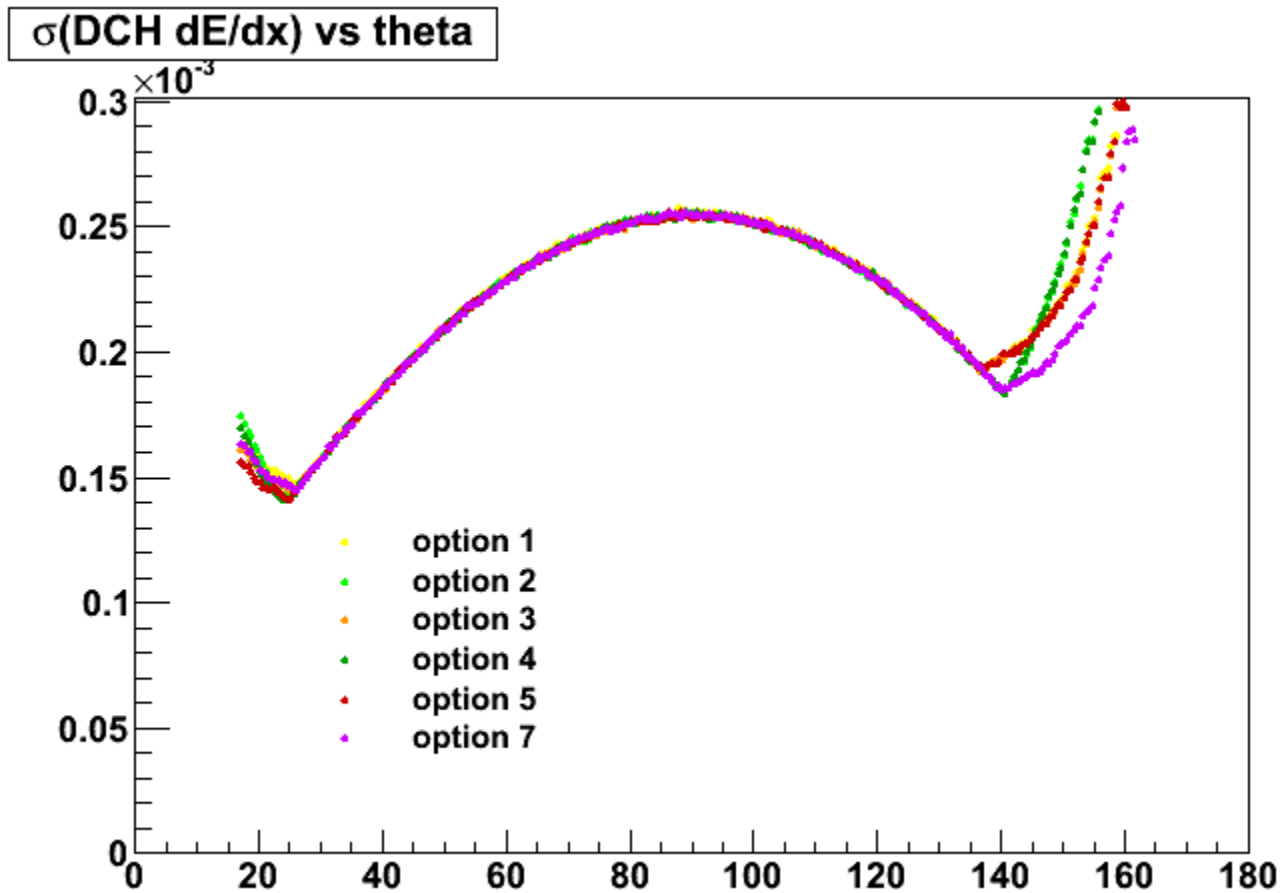


single π^+ , $p = 4\text{GeV}/c$, flat $\cos\theta$

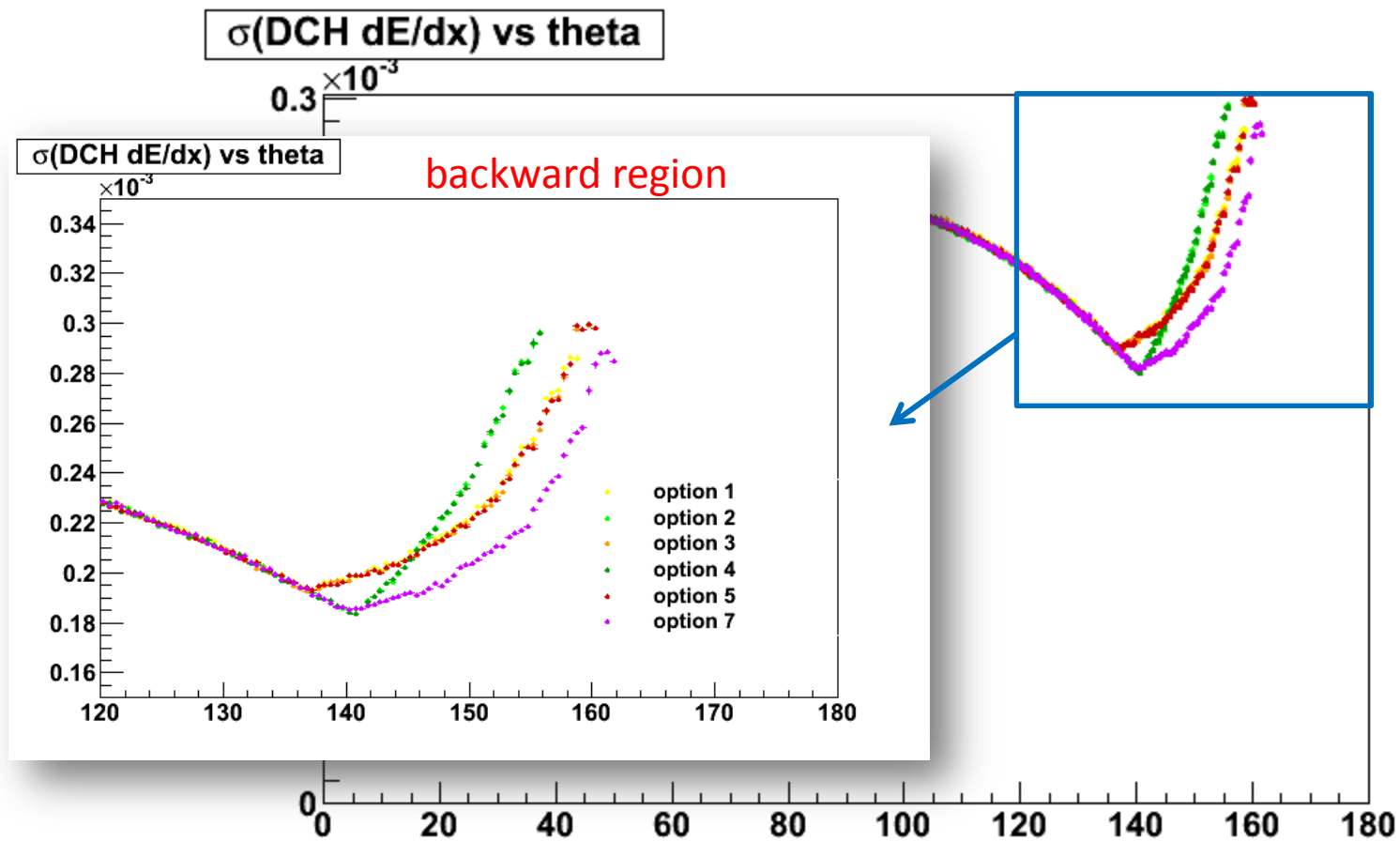
DCH dE/dx sample hits vs theta



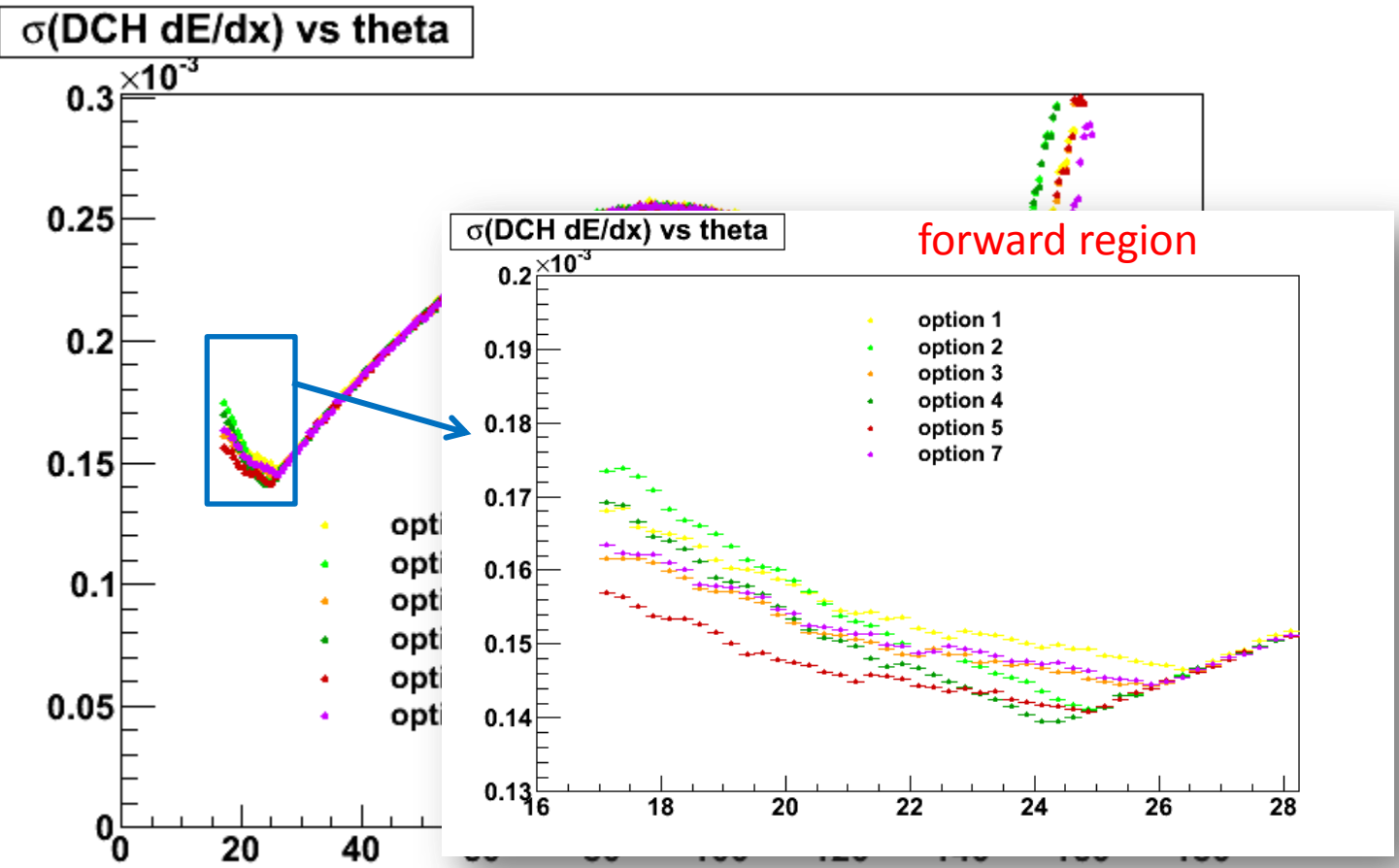
single π^+ , $p = 4\text{GeV}/c$, flat $\cos\theta$



single π^+ , $p = 4\text{GeV}/c$, flat $\cos\theta$

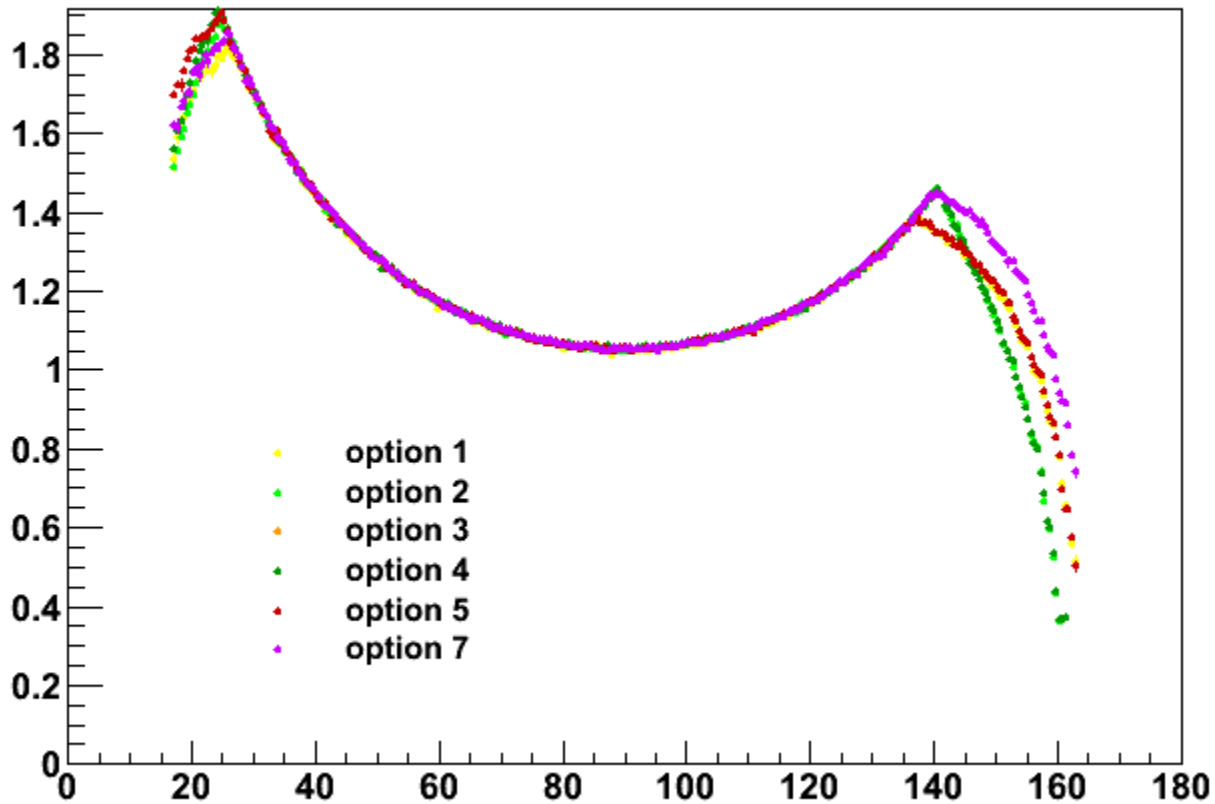


single π^+ , $p = 4\text{GeV}/c$, flat $\cos\theta$



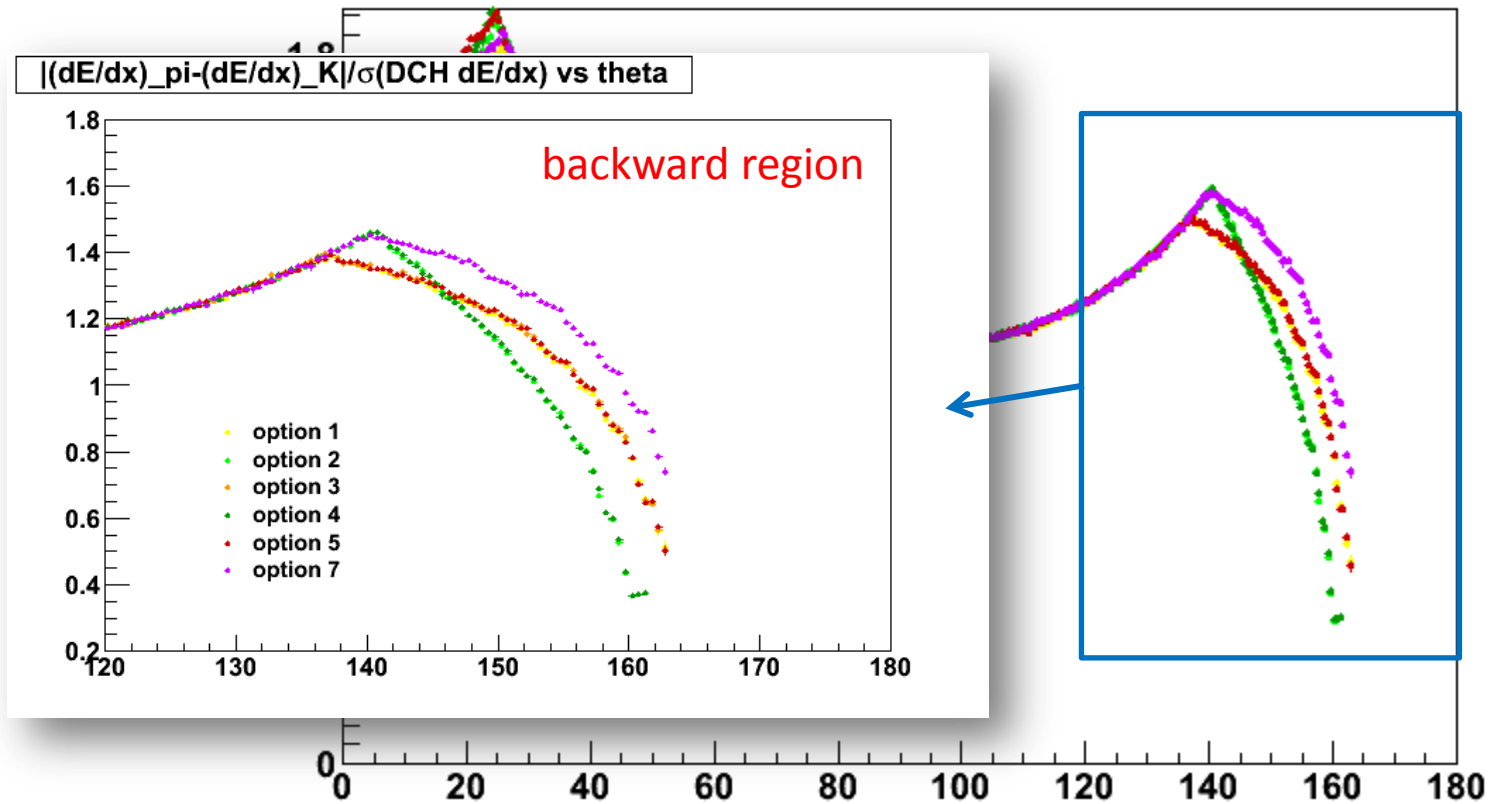
single π^+ , $p = 4\text{GeV}/c$, flat $\cos\theta$

$|(dE/dx)_{\pi} - (dE/dx)_K| / \sigma(\text{DCH } dE/dx)$ vs θ



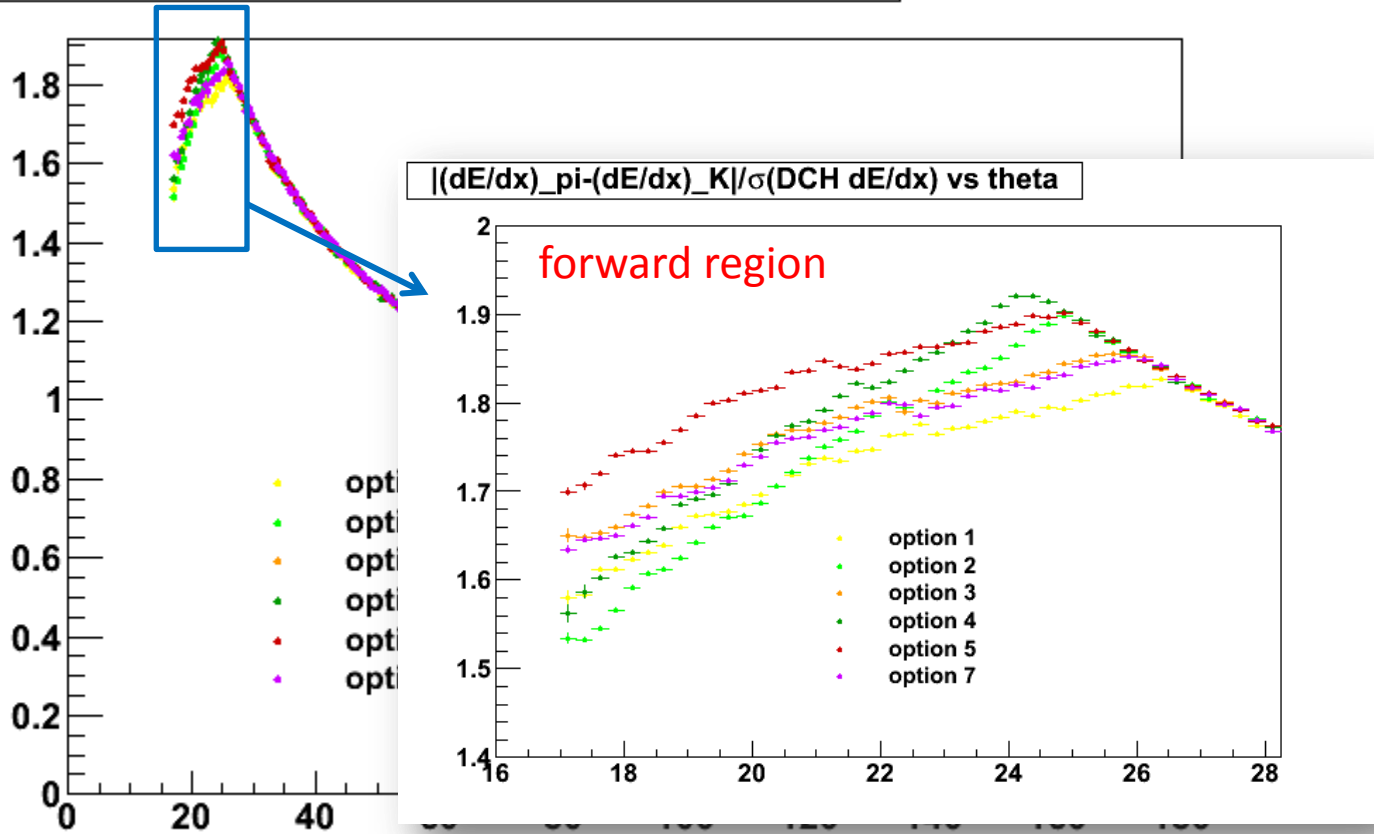
single π^+ , $p = 4\text{GeV}/c$, flat $\cos\theta$

$|(\text{dE/dx})_{\pi} - (\text{dE/dx})_{\text{K}}| / \sigma(\text{DCH dE/dx})$ vs theta



single π^+ , $p = 4\text{GeV}/c$, flat $\cos\theta$

$|(dE/dx)_{\pi} - (dE/dx)_{K}| / \sigma(\text{DCH } dE/dx)$ vs theta



Part II

single particles (π^+) with flat p and $\cos\theta$ distributions

single particles generated with:

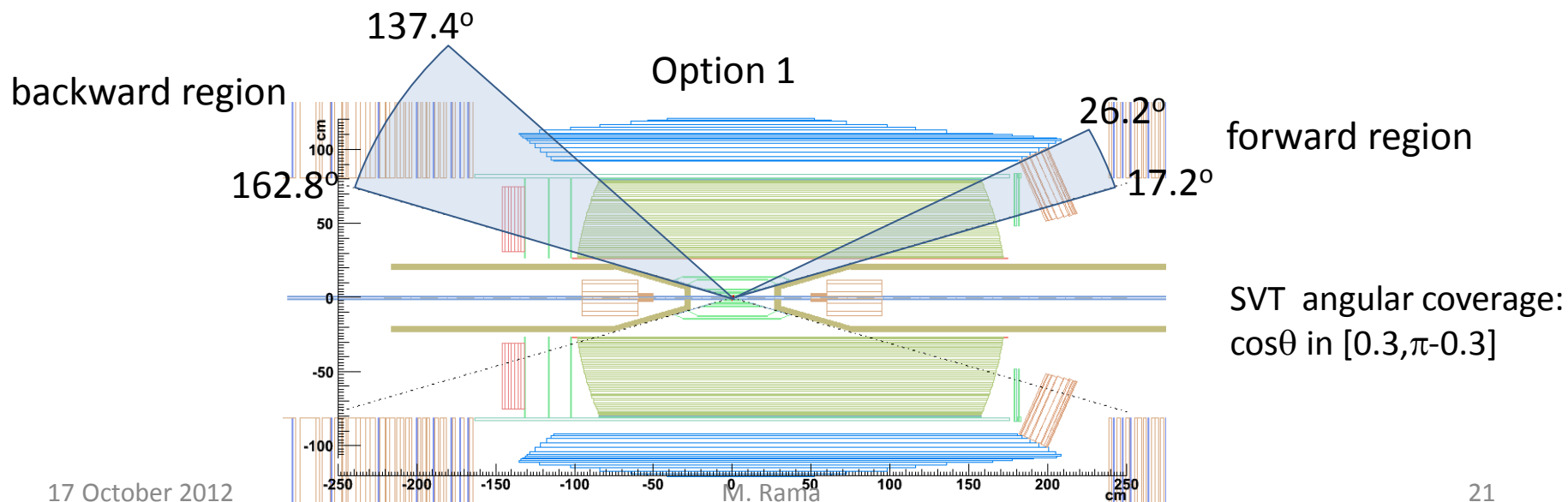
- p in $[0.1, 4.0]$ GeV/c
- $dP/d\cos\theta = \text{const}$ [θ = polar angle]
- θ in $[0.30, 0.46]$ rad [DCH forward region] or θ in $[2.40, \pi - 0.30]$ rad [DCH backward region]
- 200k events for each configuration

Part II

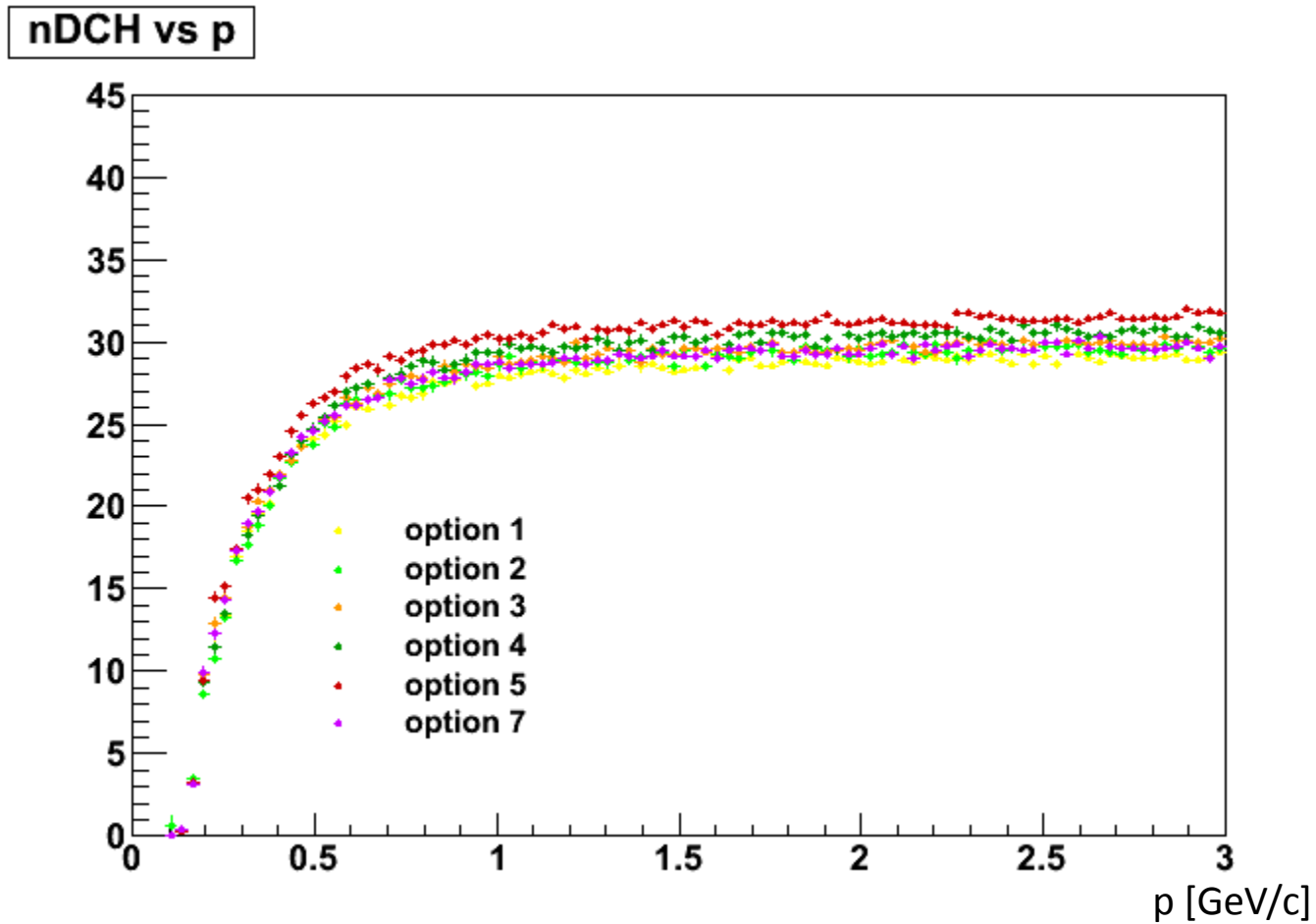
single particles (π^+) with flat p and $\cos\theta$ distributions

single particles generated with:

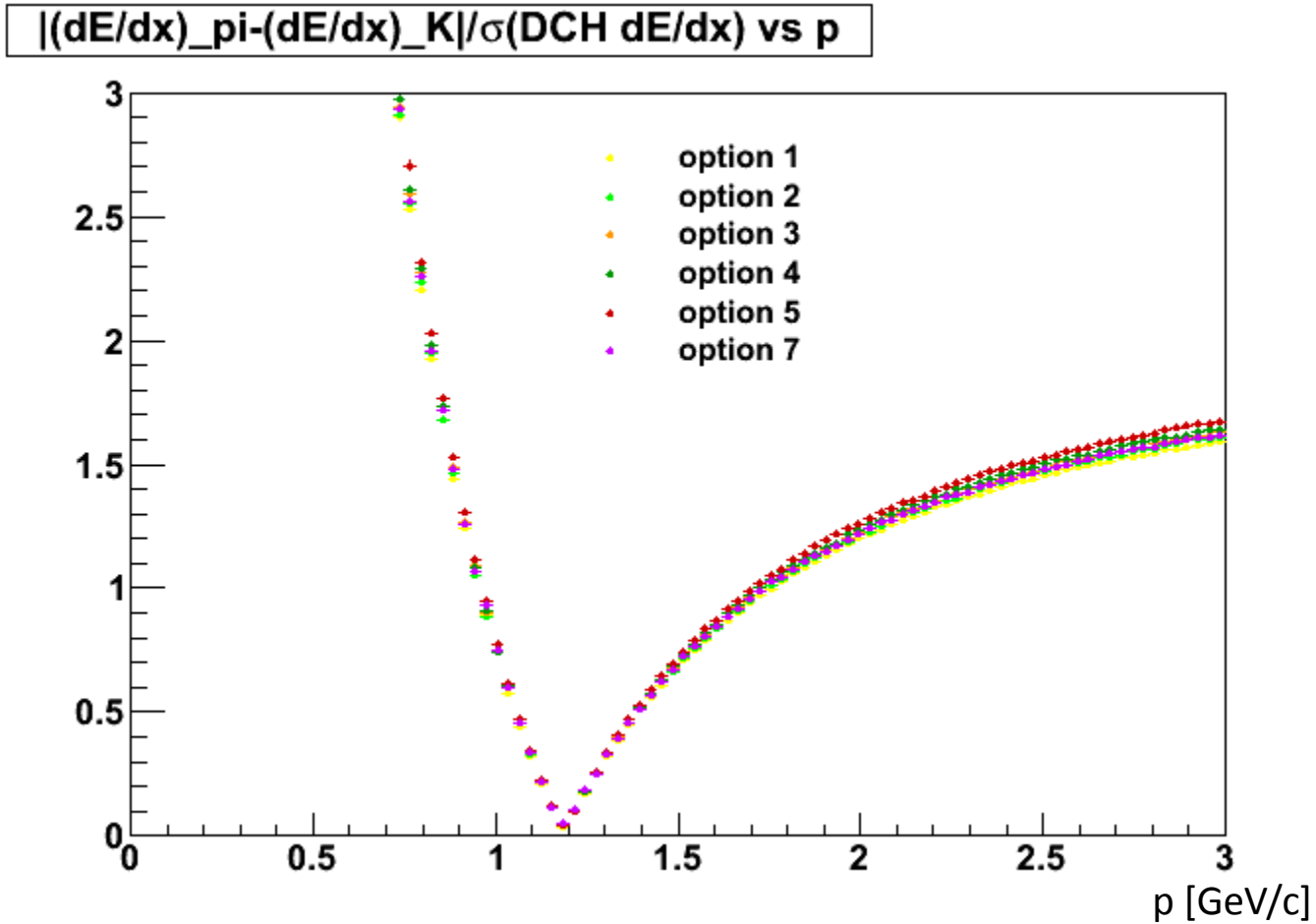
- p in $[0.1, 4.0]$ GeV/c
- $dP/d\cos\theta = \text{const}$ [$\theta = \text{polar angle}$]
- θ in $[0.30, 0.46]$ rad [DCH forward region] or θ in $[2.40, \pi - 0.30]$ rad [DCH backward region]
- 200k events for each configuration



forward region

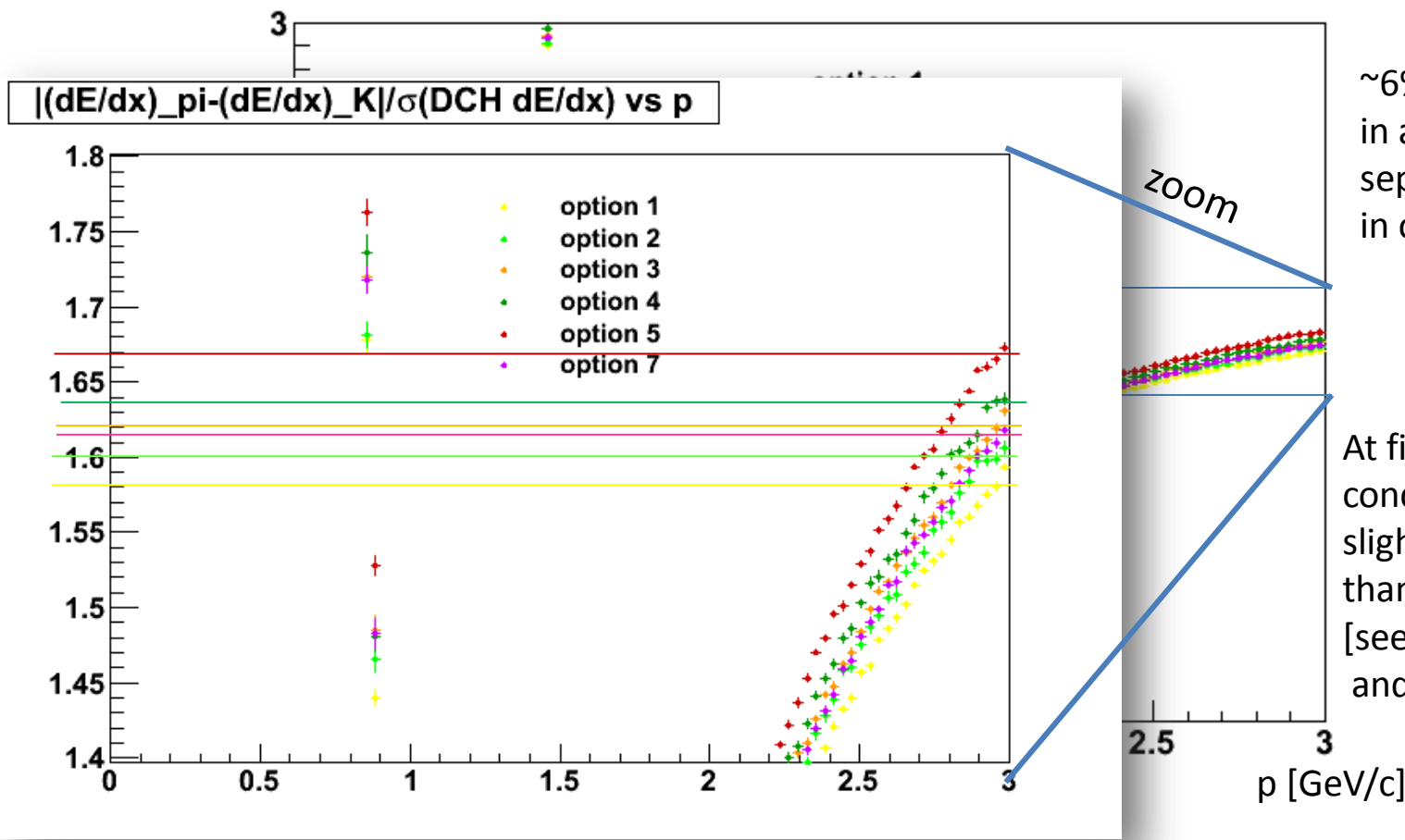


forward region



forward region

$|(dE/dx)_{\pi} - (dE/dx)_K| / \sigma(\text{DCH } dE/dx) \text{ vs } p$

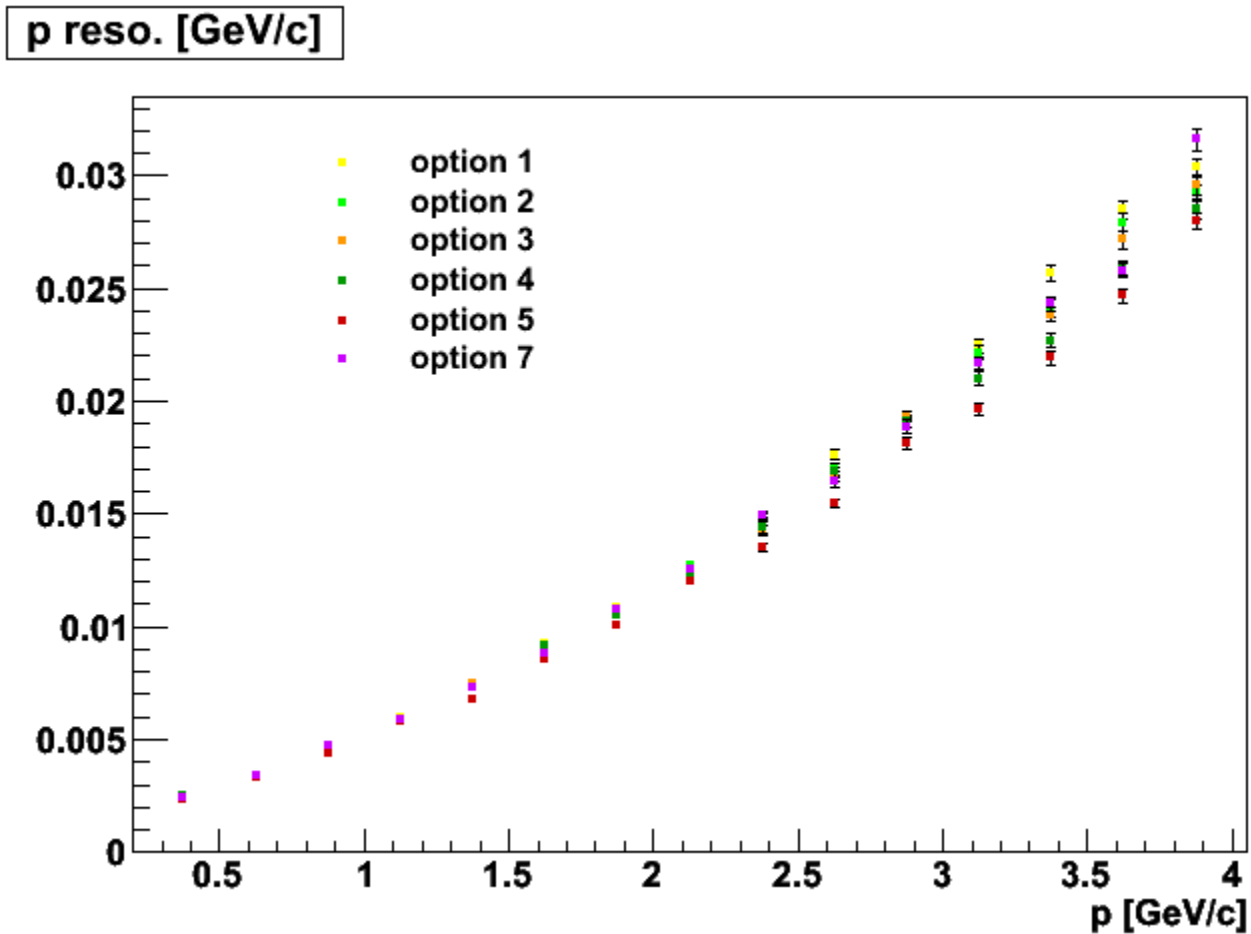


zoom

~6% variation in average K/π separation in options 1-7

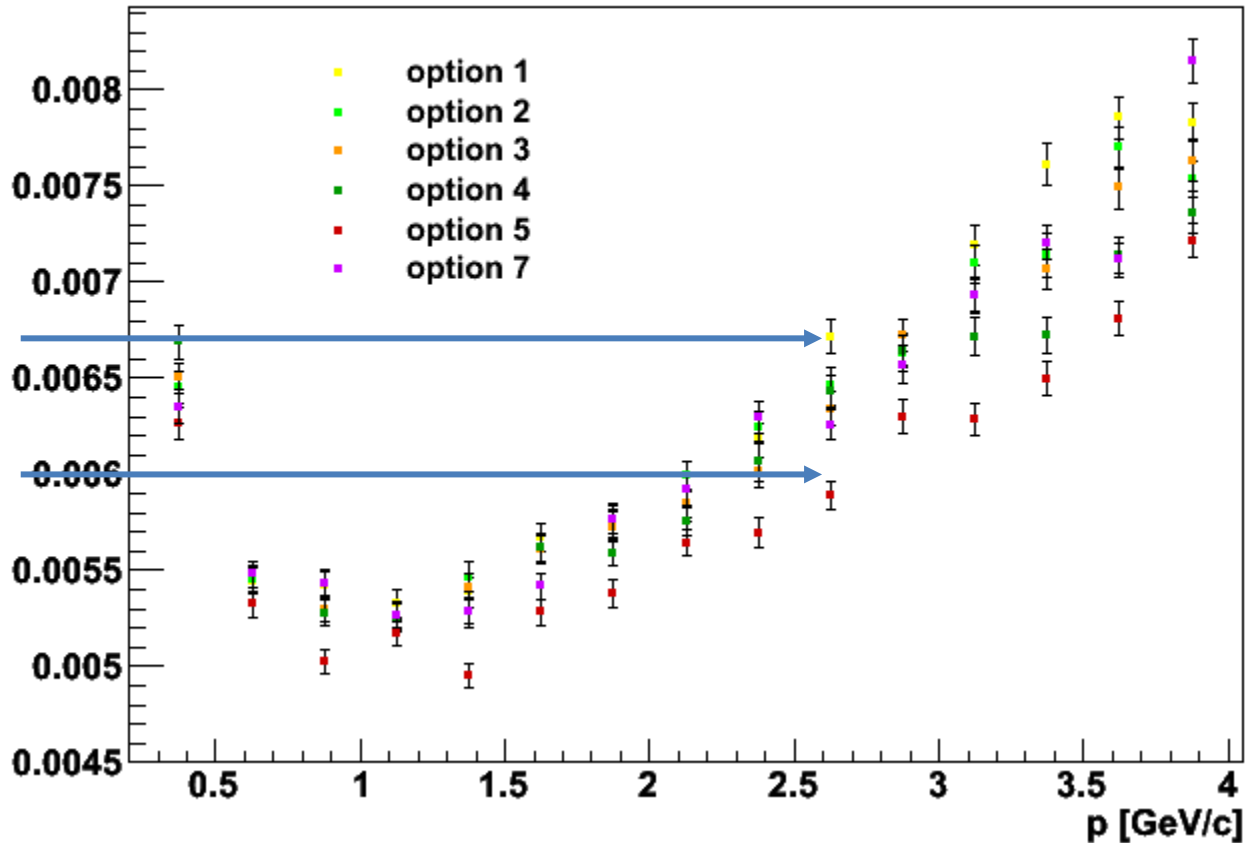
At fixed z length, concave config slightly better (~1.3%) than convex config. [see opt2 vs opt1 and opt4 vs opt3]

forward region



forward region

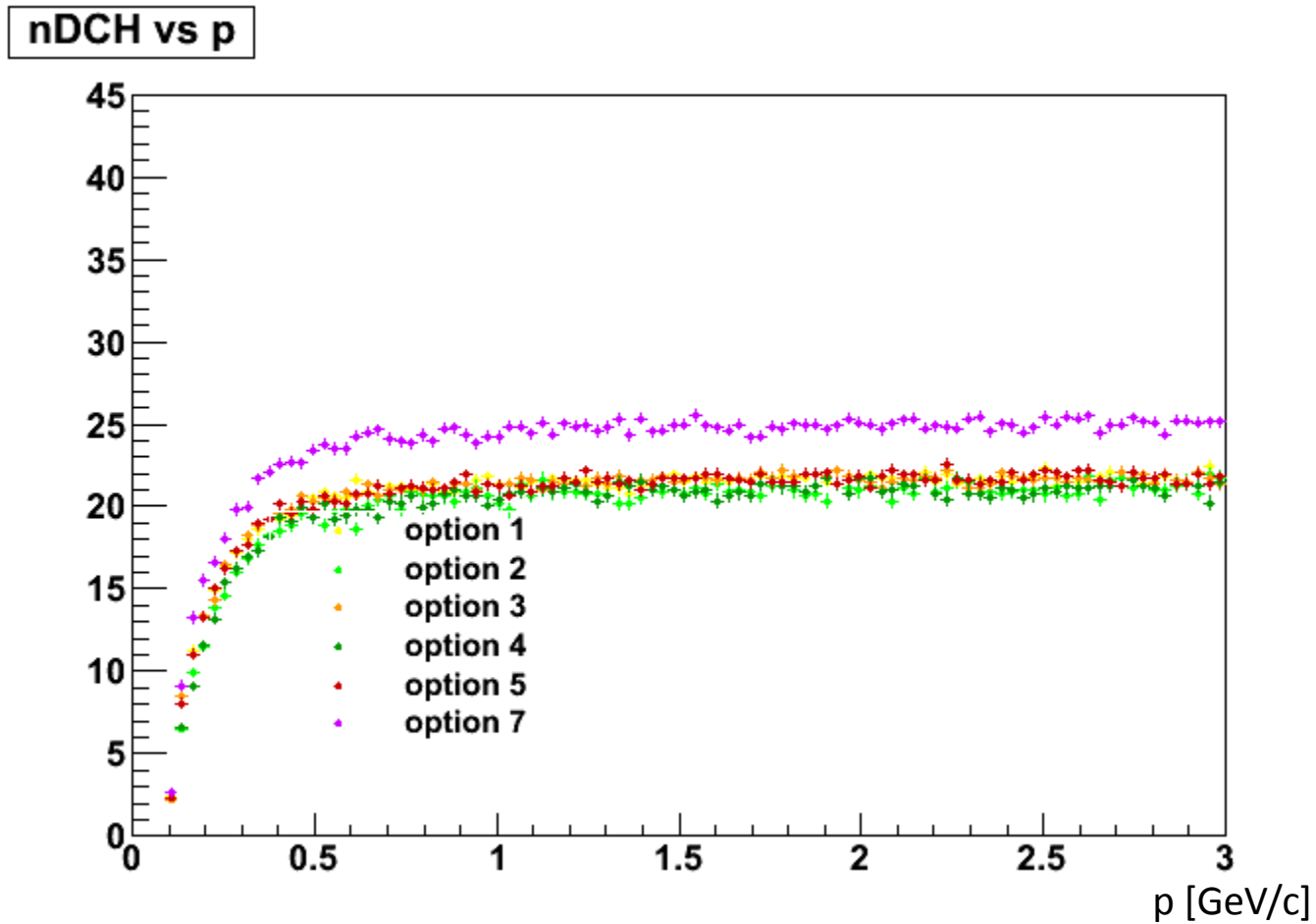
$\sigma(p)/p$ reso.



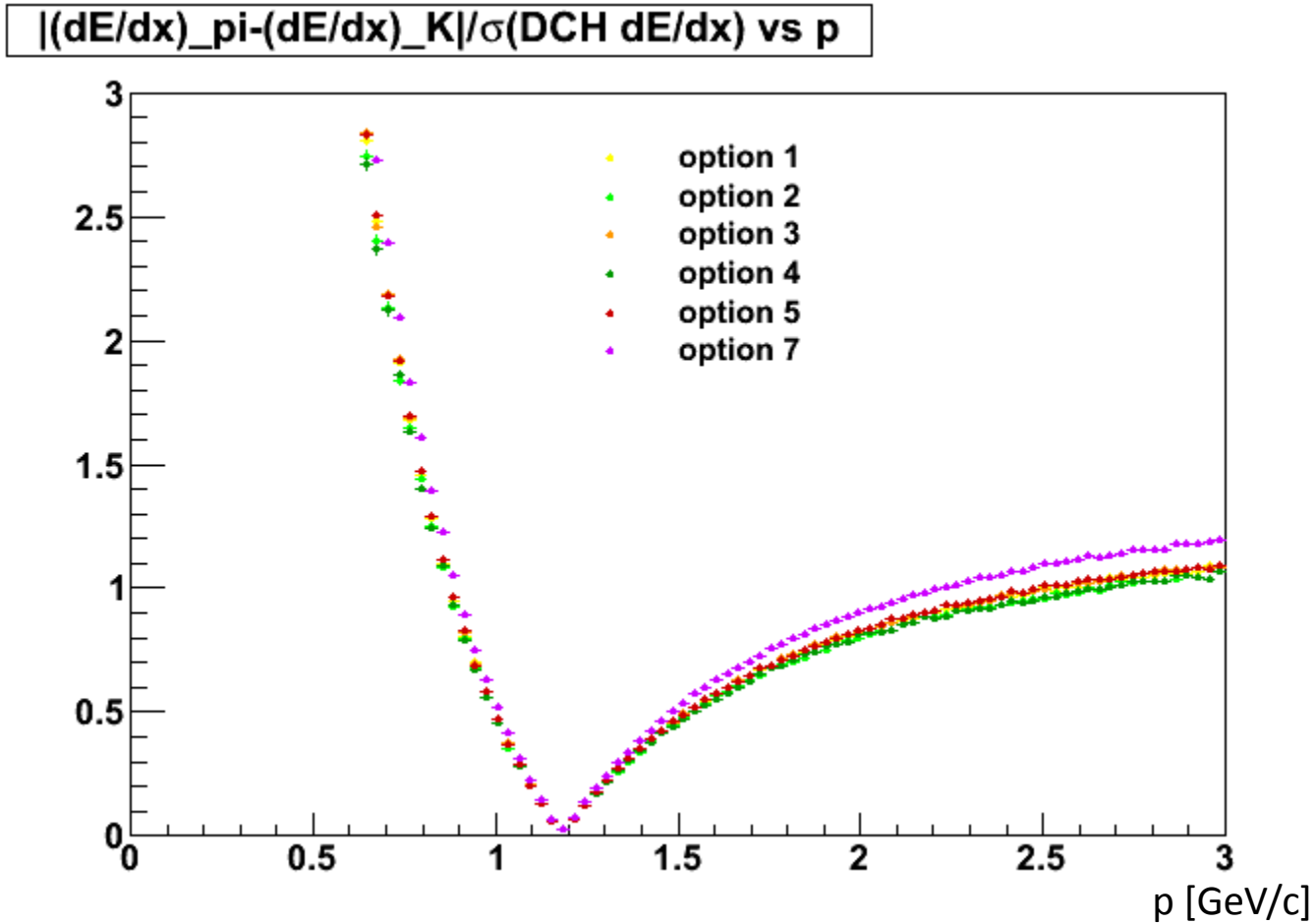
$\approx 10\%$ $\sigma(p)/p$
relative variation
over different
configs.

At fixed z length,
concave and convex
configs shows
similar performance
within the stat
uncertainty.

backward region

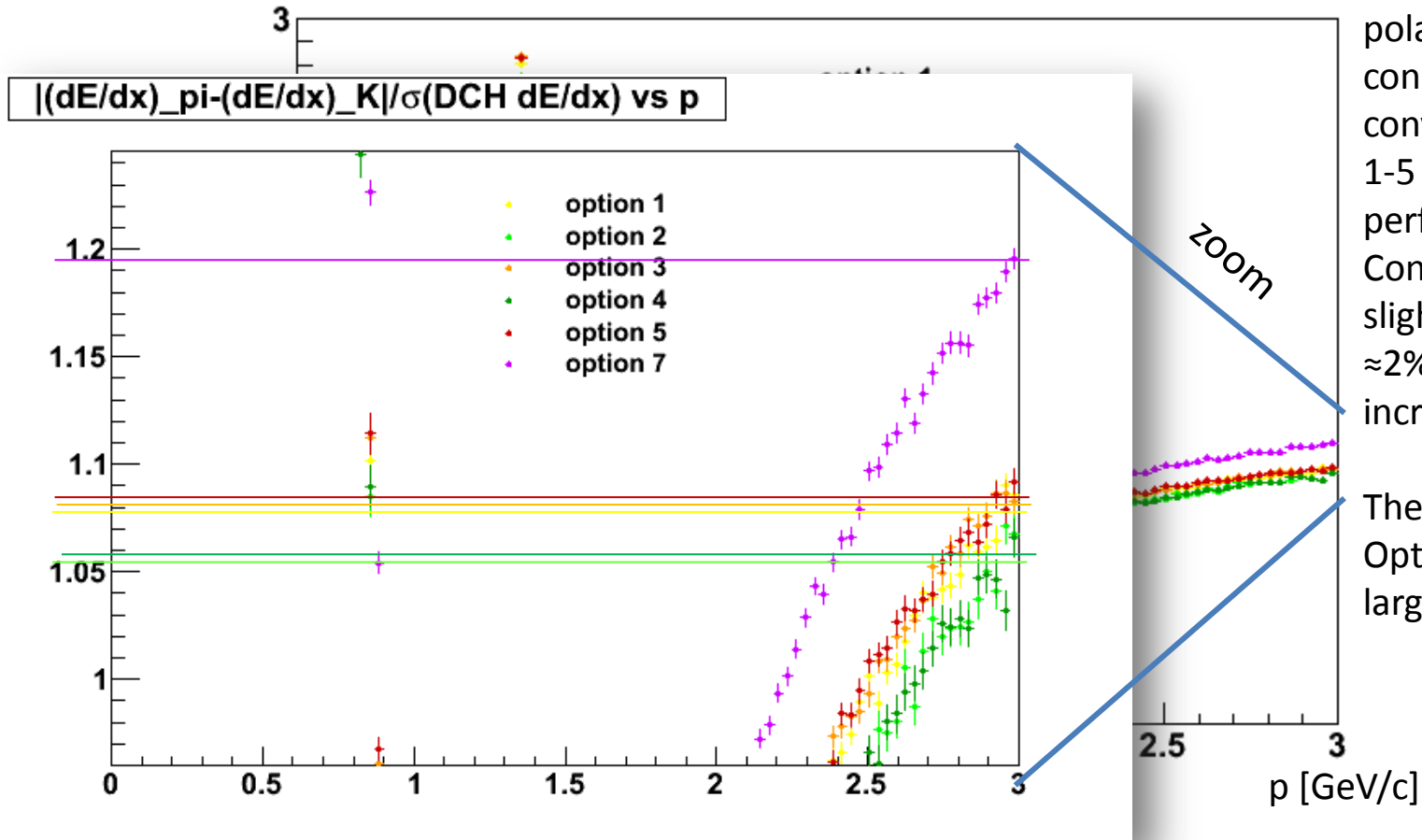


backward region



backward region

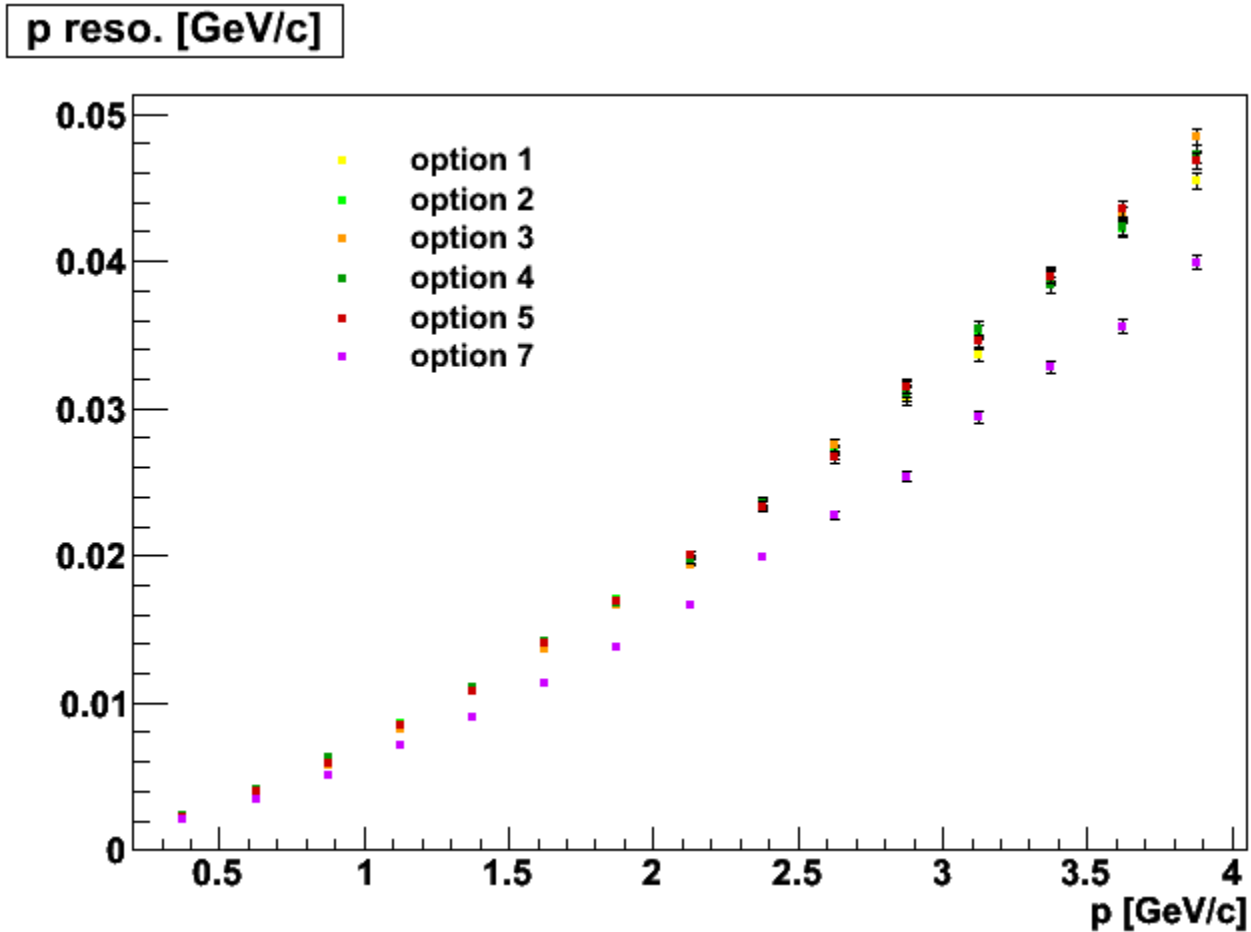
$|(dE/dx)_{\pi} - (dE/dx)_K| / \sigma(\text{DCH } dE/dx) \text{ vs } p$



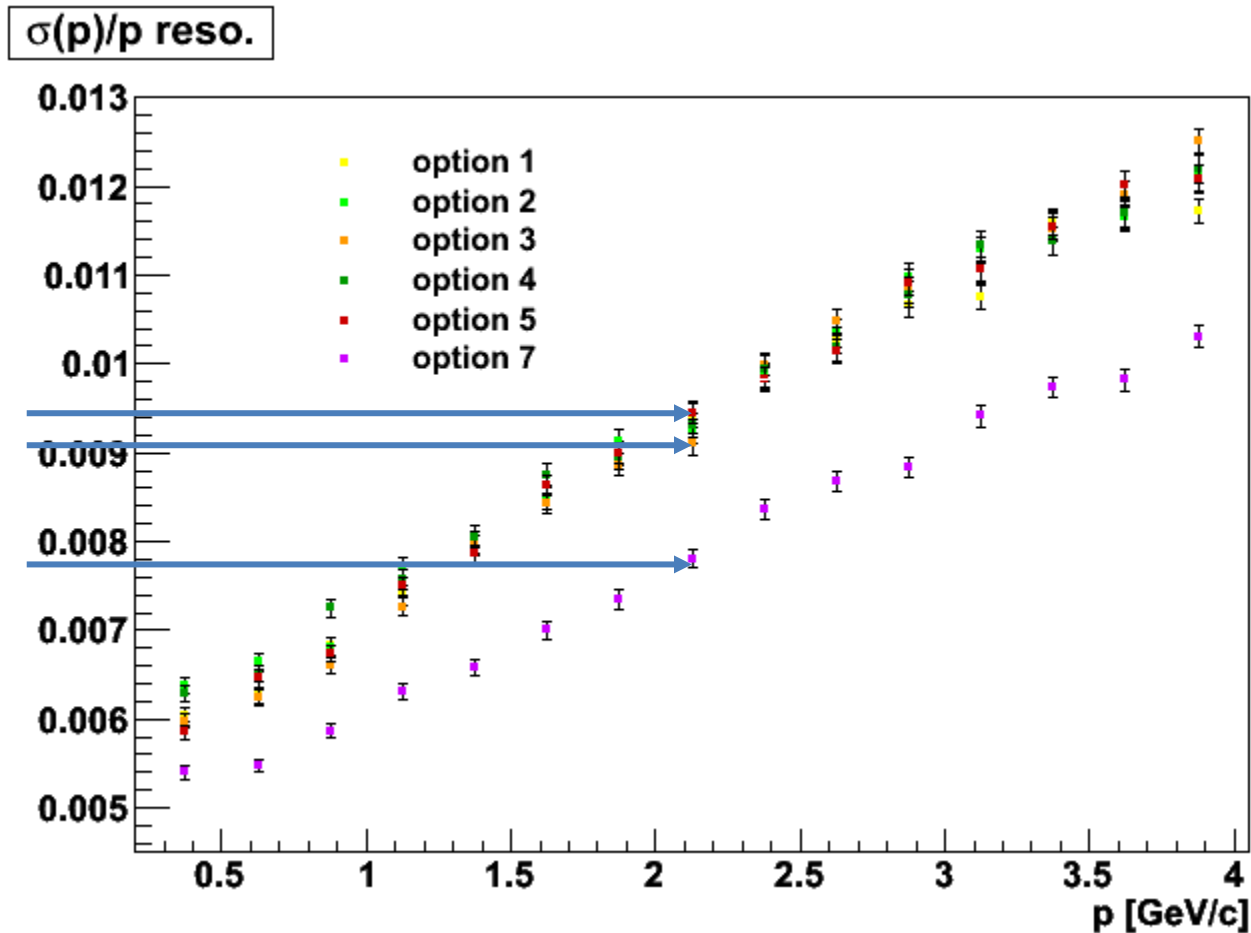
Averaged over the polar angle, the concave and convex configs 1-5 have similar performance. Convex configs slightly better: $\approx 2\%$ separation increase.

The separation of Option 7 is $\approx 10\%$ larger.

backward region



backward region



Integrated over the whole bwd region, p resolutions of Options 1-5 are similar within a $\approx 4\%$ relative variation.

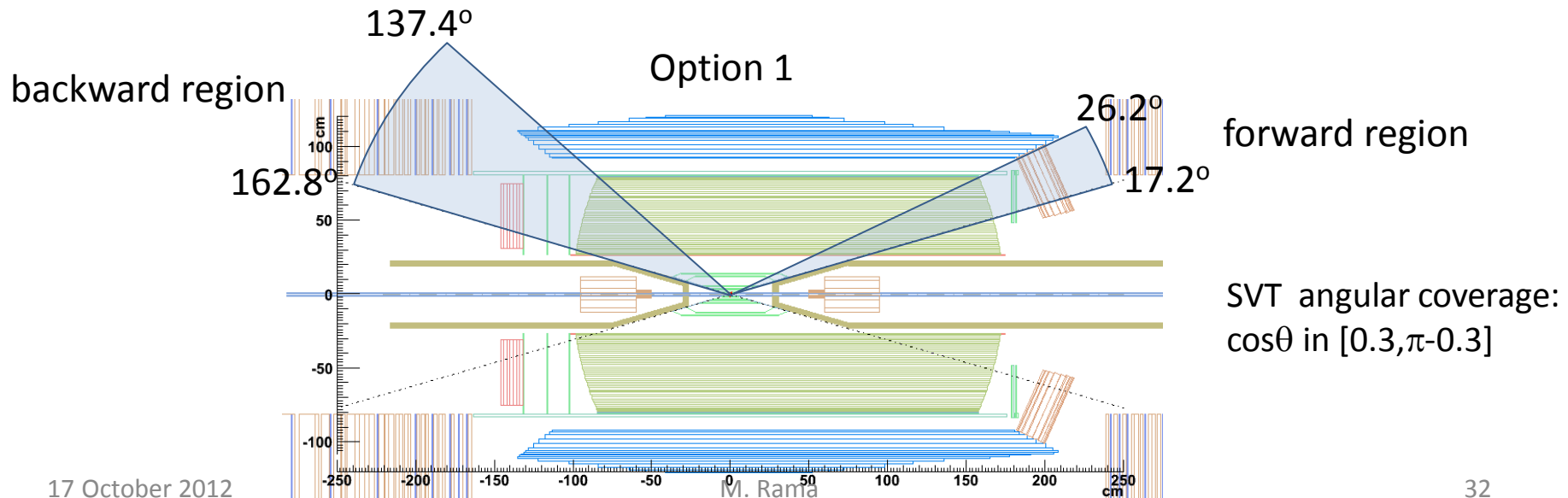
p resolution of Option 7 is $\approx 15-20\%$ better.

Part III

$$B^0 \rightarrow D^{*-} K^+, D^{*-} \rightarrow \bar{D}^0 K^-, \bar{D}^0 \rightarrow K^+ \pi^-$$

5×10^4 $B \rightarrow D^* K$ signal events for each configuration

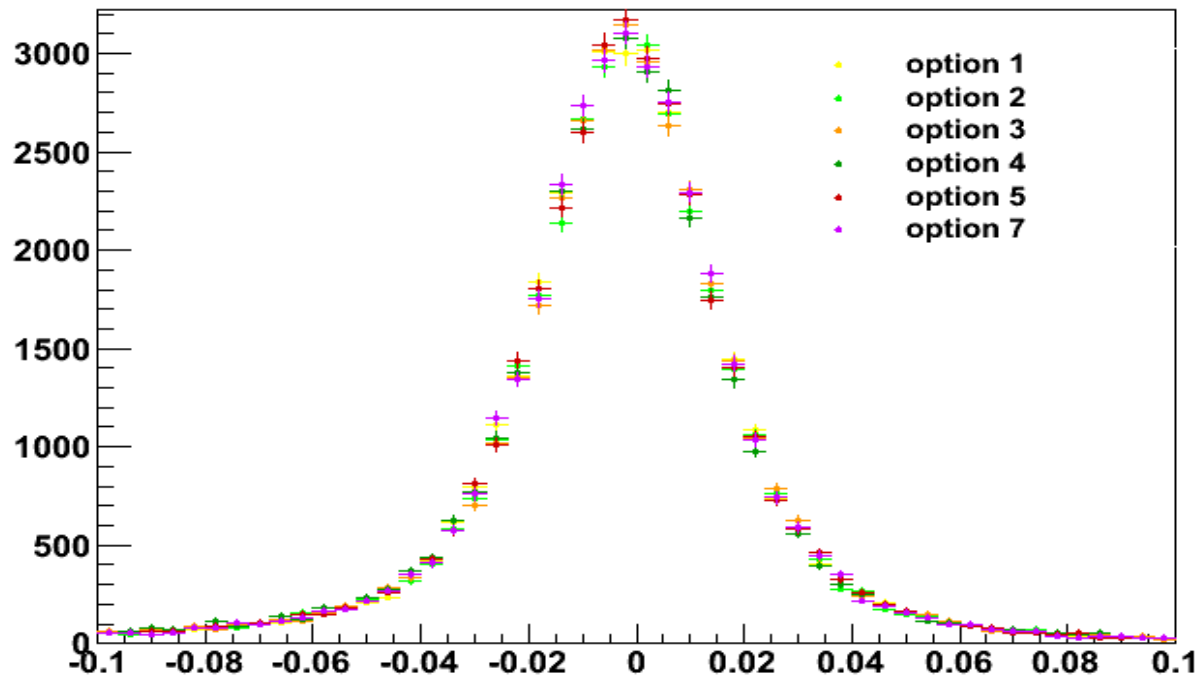
- truth matching required



ΔE reconstruction

$$B^0 \rightarrow D^{*-}K^+, D^{*-} \rightarrow \bar{D}^0K^-, \bar{D}^0 \rightarrow K^+\pi^-$$

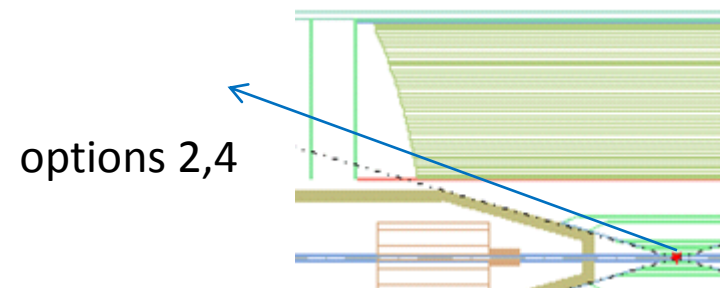
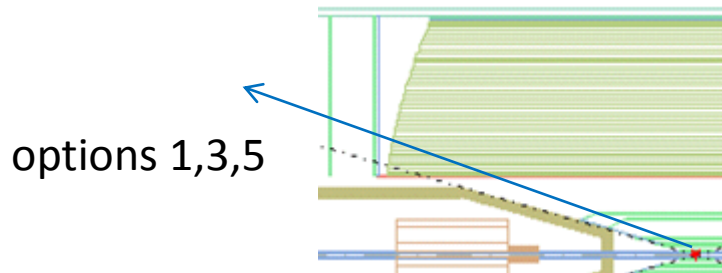
DeltaE



reconstruction efficiency of $B \rightarrow D^* K$

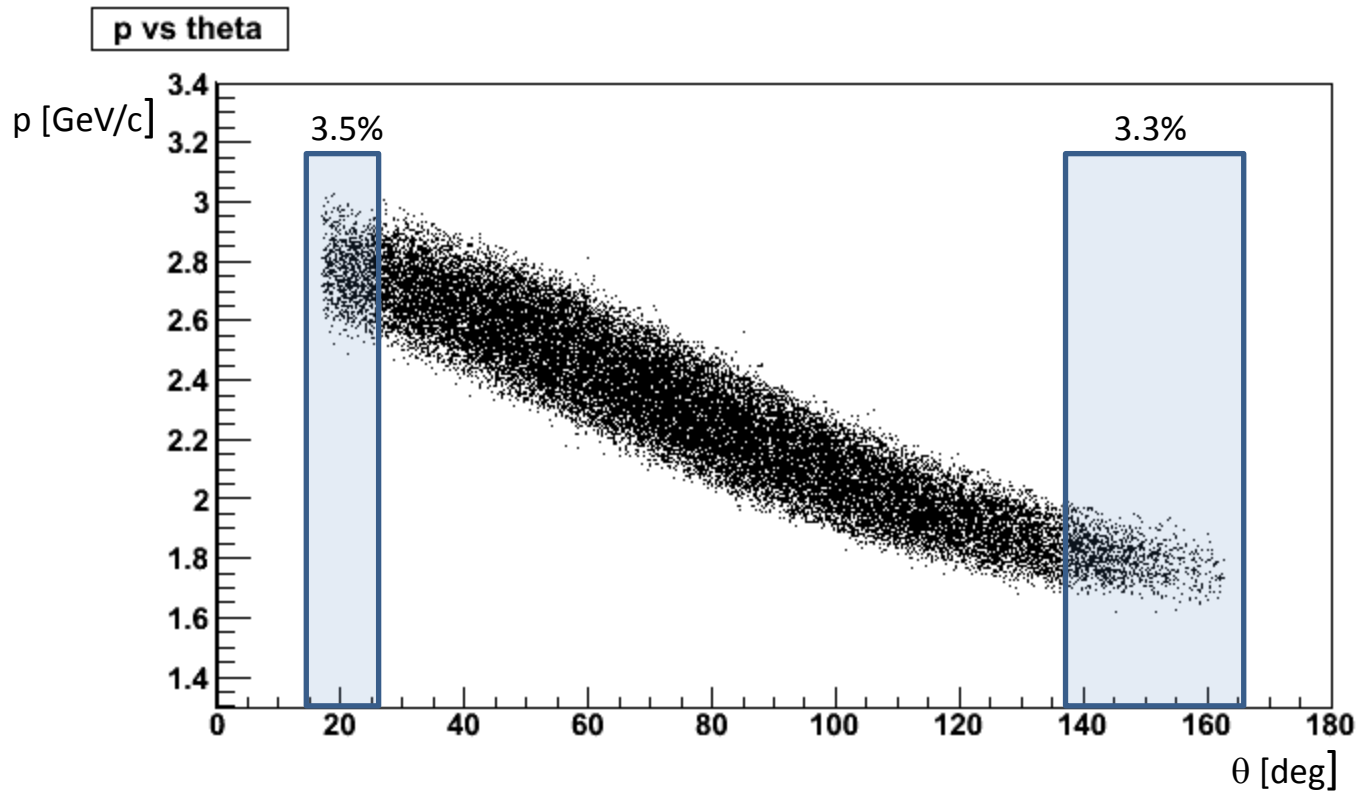
DCH configuration	$B \rightarrow D^* K$ reco efficiency [%] ($ \Delta E < 50 \text{ MeV} \sim 2.5\sigma$)
option 1	65.4 ± 0.2
option 2	64.4 ± 0.2
option 3	65.1 ± 0.2
option 4	64.6 ± 0.2
option 5	65.3 ± 0.2
option 7	65.6 ± 0.2

The (tiny) differences are driven by the backward region: $\text{eff}[\text{opt}1,3,5,7] > \text{eff}[\text{opt}2,4]$



Options 1, 2, 3 and 7 have the same efficiency within $\approx 0.2\%$

p vs θ distribution of prompt kaons ($B \rightarrow D^* K$)

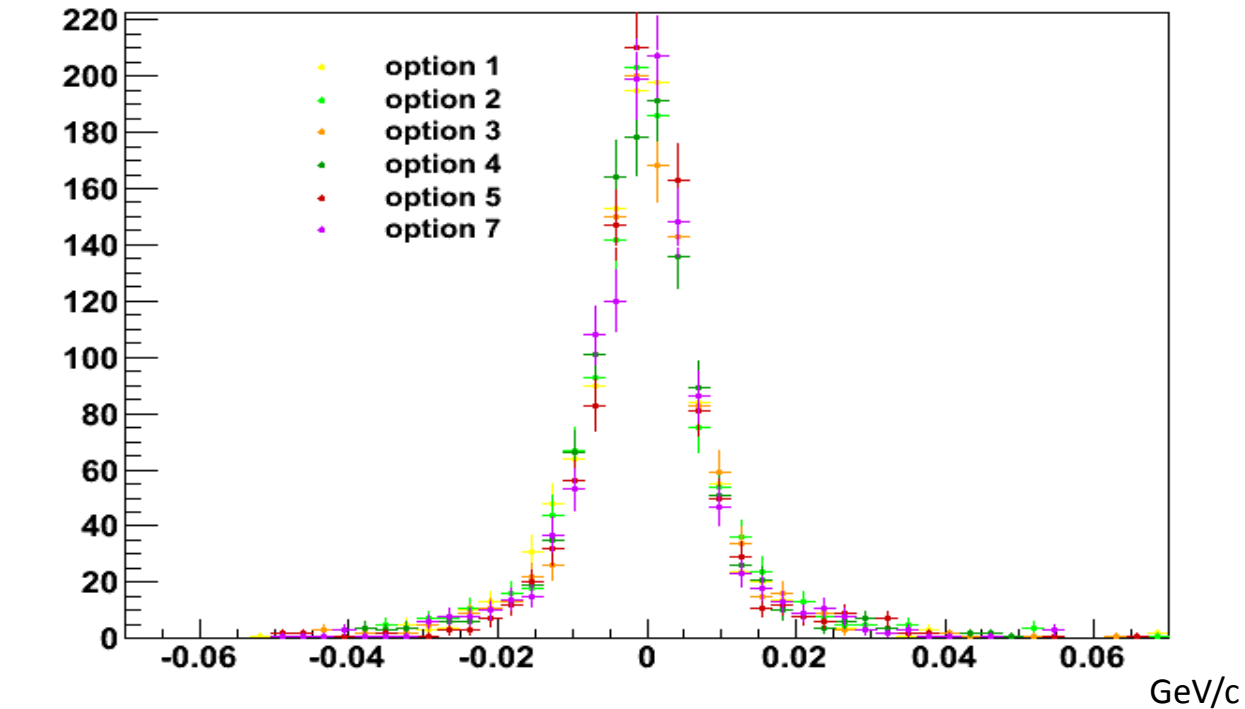


selected samples

forward region: 1213 (3.5%)
barrel region: 32242 (93.2%)
backward region: 1157 (3.3%)

forward region

pt reso for prompt kaons in forward region



Option 5 is visibly better.
Differences in the other options are not evident.

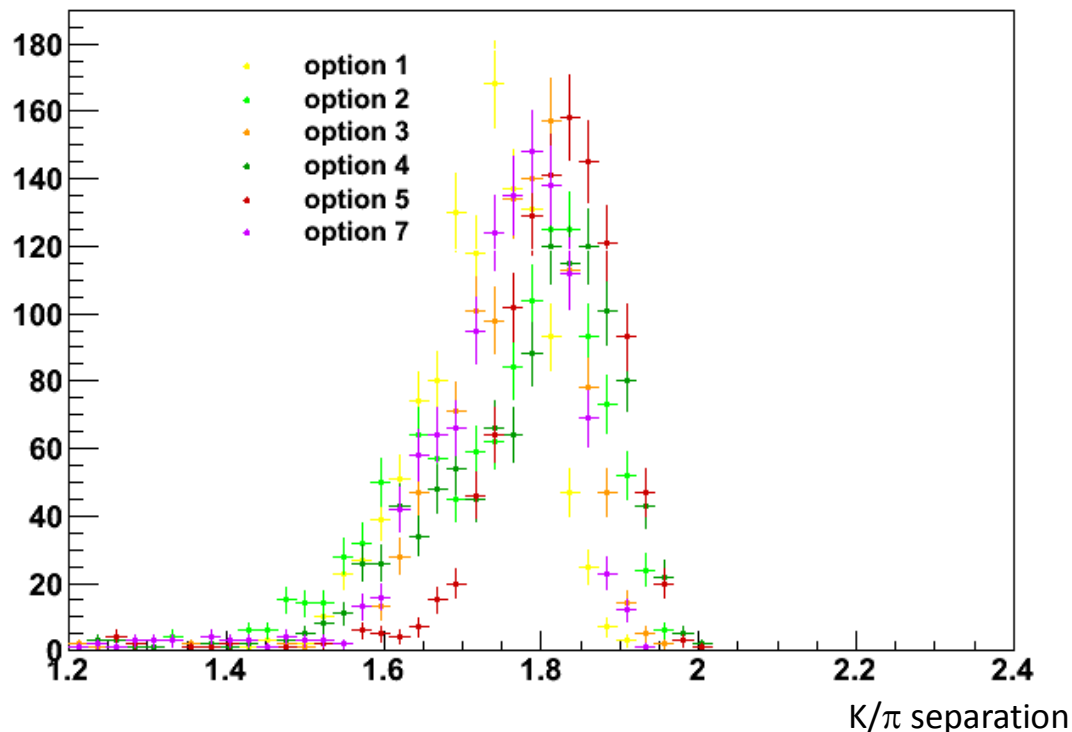
forward region

$$K/\pi \text{ separation} \equiv \frac{|(dE/dx)_\pi - (dE/dx)_K|}{\sigma(dE/dx)}$$

$(dE/dx)_h =$ expected dE/dx in the h hypothesis

$\sigma(dE/dx) =$ dE/dx measurement error

$|(\text{dE/dx})_\pi - (\text{dE/dx})_K| / \sigma(\text{DCH dE/dx})$ forward



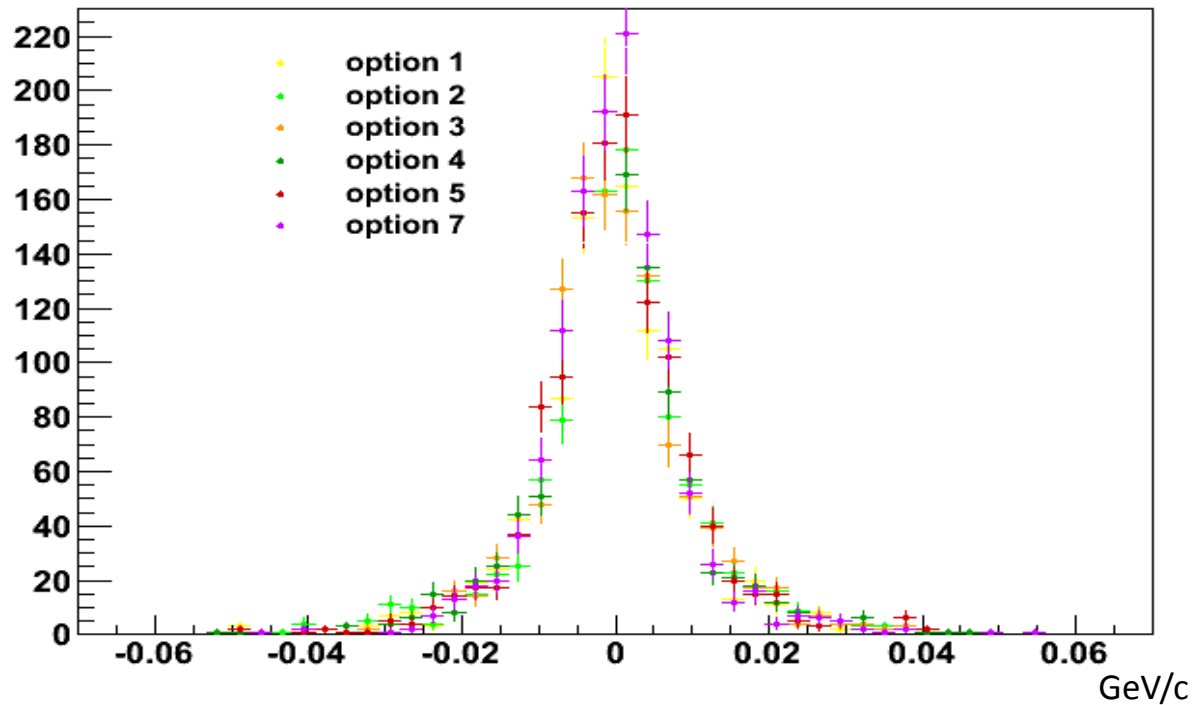
config	$\mu \pm \text{RMS}/\sqrt{N}$
1	1.723 ± 0.002
2	1.751 ± 0.003
3	1.767 ± 0.003
4	1.787 ± 0.003
5	1.822 ± 0.003
7	1.757 ± 0.003

The pattern $sep1 < sep2 < sep3 < sep4 < sep5$ is visible. Differences are tiny.

At fixed z length, concave config slightly better ($\approx 1\%$) than convex config.
[see opt2 vs opt1 and opt4 vs opt3]

backward region

pt reso pt resolution for prompt kaons in backward region



backward region

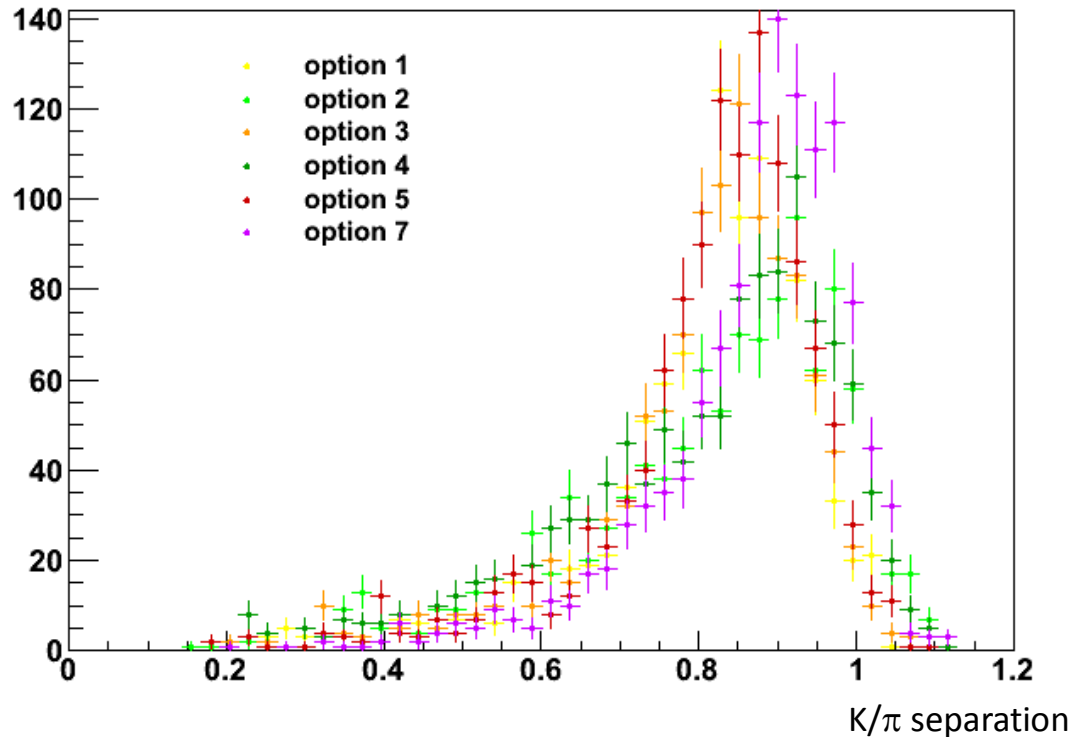
$$K/\pi \text{ separation} \equiv \frac{|(dE/dx)_\pi - (dE/dx)_K|}{\sigma(dE/dx)}$$

$(dE/dx)_h =$ expected dE/dx in the h hypothesis

$\sigma(dE/dx) =$ dE/dx measurement error

config	$\mu \pm RMS/\sqrt{N}$
1	0.801 ± 0.004
2	0.812 ± 0.005
3	0.802 ± 0.004
4	0.808 ± 0.005
5	0.816 ± 0.004
7	0.870 ± 0.004

$|dE/dx_\pi - dE/dx_K| / \sigma(DCH \text{ } dE/dx)$ backward



Average K/π separations of Opt 1-5 consistent within $\approx 0.5\%$.

K/π separation of Opt 7 is $\approx 7-8\%$ larger.

Conclusions (Options 1-5)

- 5 options for the DCH endcaps have been compared. They differ in shape and z position.
- Differences in performance are generally small, as expected.
- **Forward region**
 - K/ π separation: At fixed z position, the concave shape shows slightly better performance ($\approx 1\%$ relative gain).
 - p resolution: $\approx 10\%$ $\sigma(p)/p$ variation over different configs. Consistent with previous estimates of $\approx 1\%$ per cm of DCH length[1]. At fixed z length, concave and convex configs shows similar performance within the stat uncertainty (2-3%).
 - B \rightarrow D*K: Possible differences in absolute (relative) reco efficiency due to track reconstruction and ΔE resolution are below 0.2% (0.3%) among different configs.
- **Backward region**
 - K/ π separation: Using single particles generated with flat $\cos\theta$ and p distributions, and averaging over the bwd region, the convex configuration shows slightly better performance ($\approx 2\%$). Using prompt kaons from B \rightarrow D*K, concave and convex configurations are consistent within 0.5%.
 - p resolution: Integrated over the whole bwd region, p resolutions are equal within a $\approx 4\%$ relative uncertainty.
 - B \rightarrow D*K: convex configuration shows slightly larger B \rightarrow D*K reco efficiency: 0.8% (1.2%) absolute (relative) efficiency gain.

[1] <http://agenda.infn.it/getFile.py/access?contribId=74&sessionId=11&resId=0&materialId=slides&confId=2902>

[2] <http://agenda.infn.it/getFile.py/access?contribId=133&sessionId=19&resId=0&materialId=slides&confId=1165>

convex vs concave shape summary (Options 1-5)

Summary of results concerning the comparison between the concave and convex shapes with a given length (i.e., option1 vs option2 or option3 vs option4)

	forward region	backward region
K/π separation	concave +1% w.r.t. convex	With single particles (flat $\cos\theta$): convex +2% w.r.t. concave With prompt K from $B \rightarrow D^*K$: same separation within 0.5%. (*)
$\sigma(p)/p$	same resolution within 2-3% relative uncertainty (stat limited)	same resolution within $\approx 4\%$ relative uncertainty (stat limited)
$B \rightarrow D^*K$ reco. eff.	same reco. eff. within 0.3% relative uncertainty (stat limited)	convex +1.2% relative increase w.r.t. concave

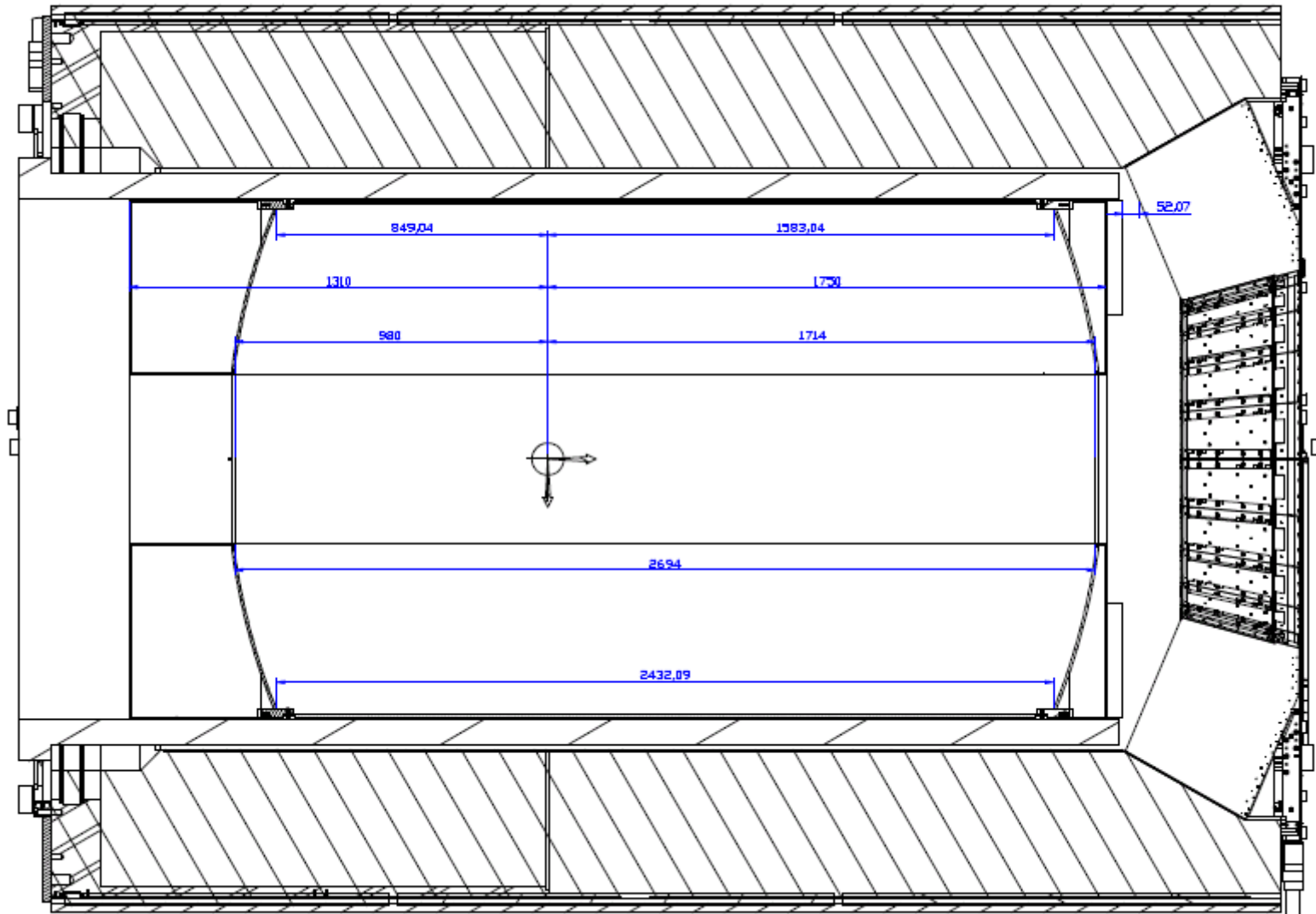
(*) The K/π separation depends on both the polar angle (see for example slide 17) and p . Therefore, results for particle samples with different polar angle and p distributions can vary.

Conclusion (Option 7 vs 1-5)

- **Backward region**
 - K/π separation in Option 7 is about 10% larger than that in Options 1-5.
 - p resolution in Option 7 is about 15-20% better than in Options 1-5.
 - $B \rightarrow D^* K$ reco efficiency in Option 7 is consistent with that in Options 1,3,5 within 0.2%.
- **Forward region**
 - Options 7 and 3 have the same performance

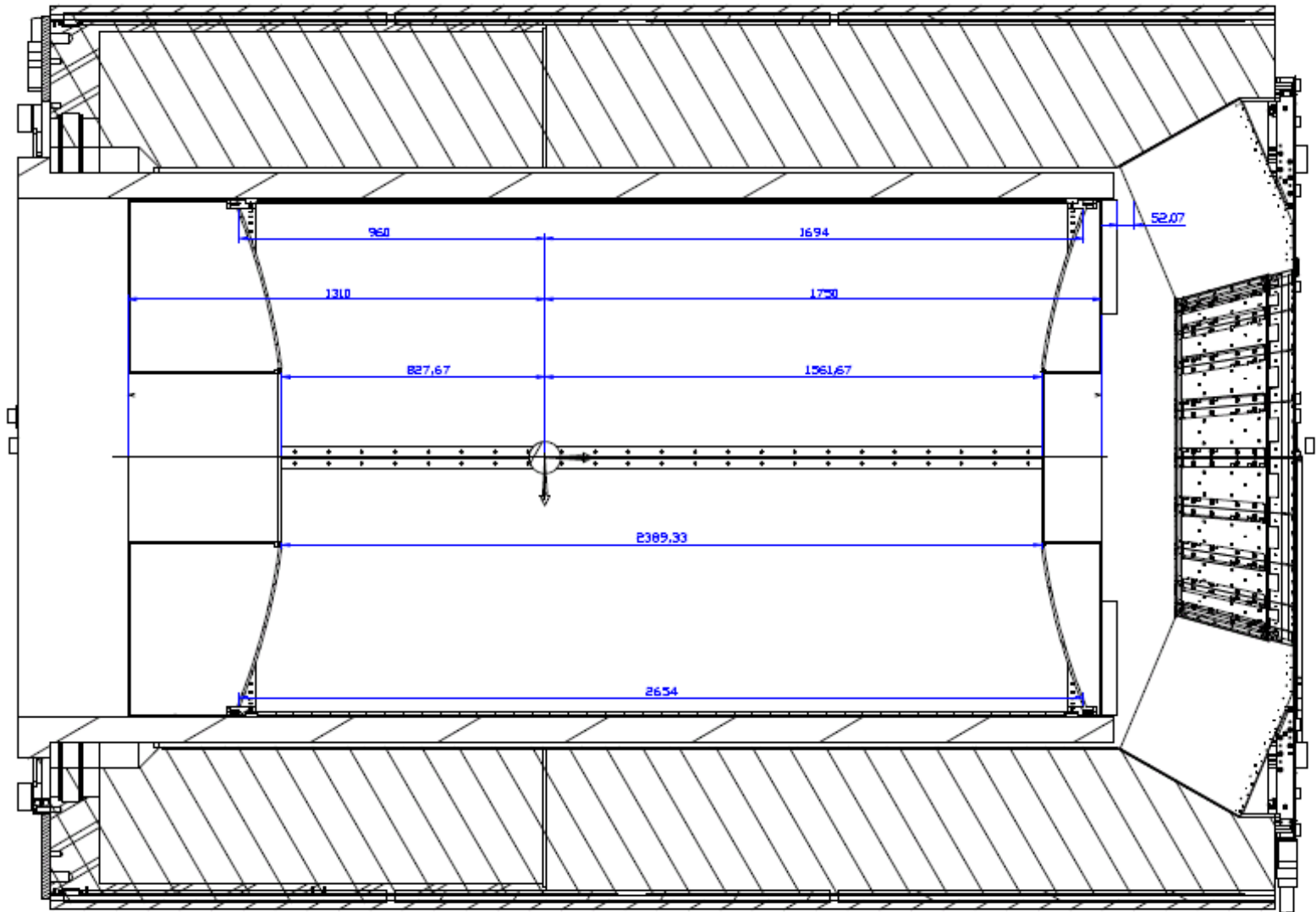
backup

1) CONVEX dimensions -1310 +1750



Drawing from Stefano Lauciani, LNF

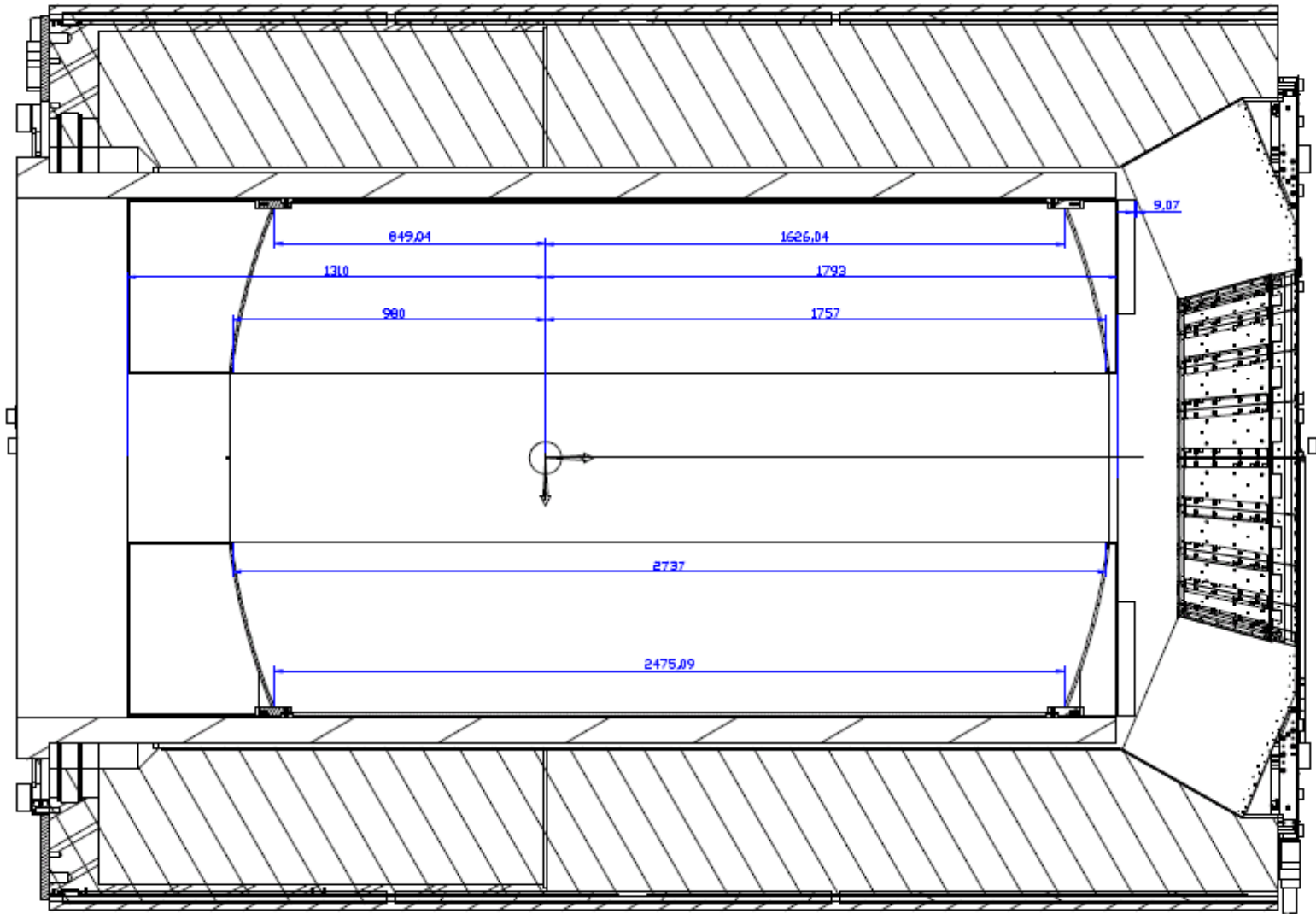
2) CONCAVE dimensions -1310 +1750



Drawing from Stefano Lauciani, LNF

210 mm

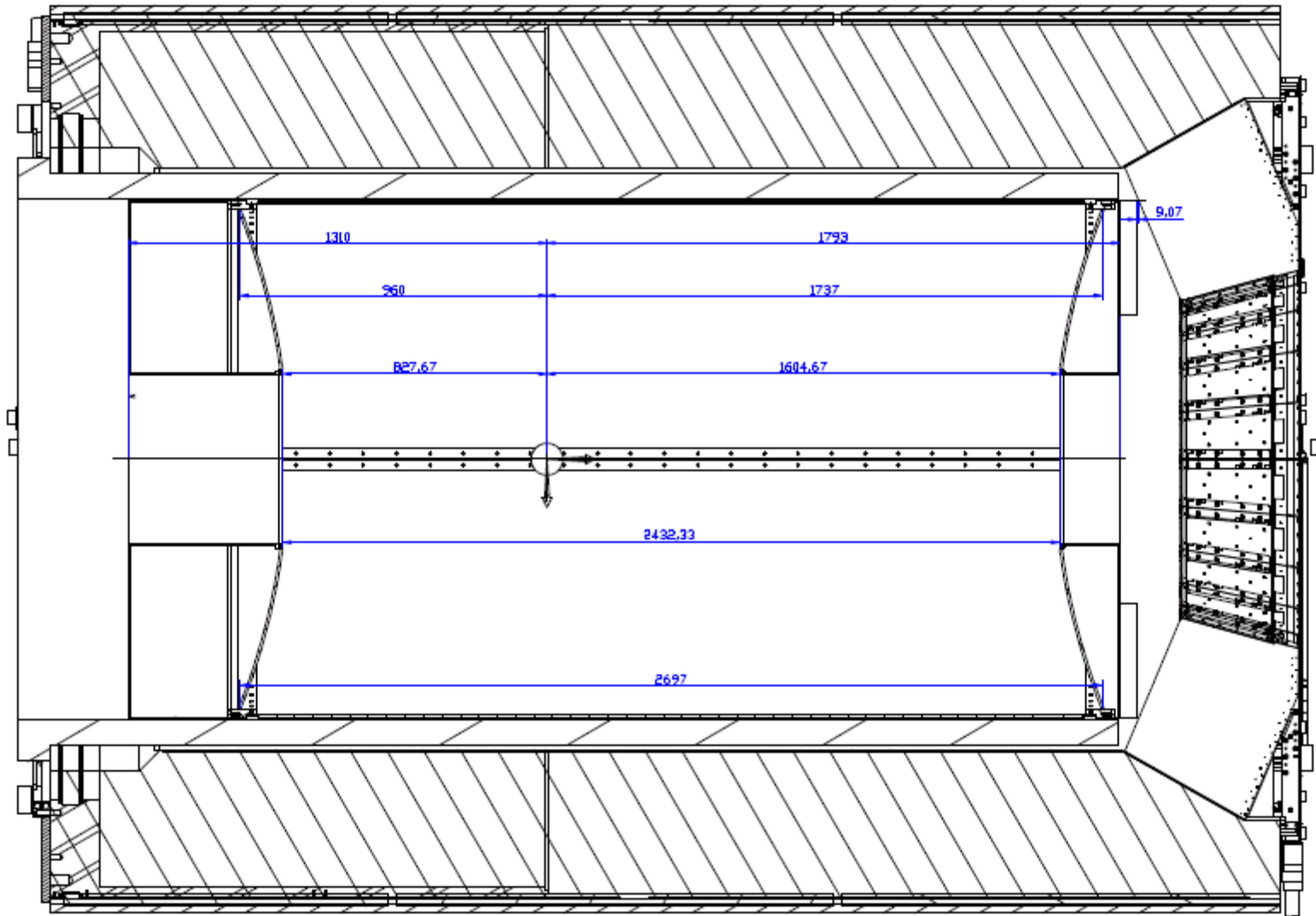
3) CONVEX dimensions -1310 +1793



210 mm

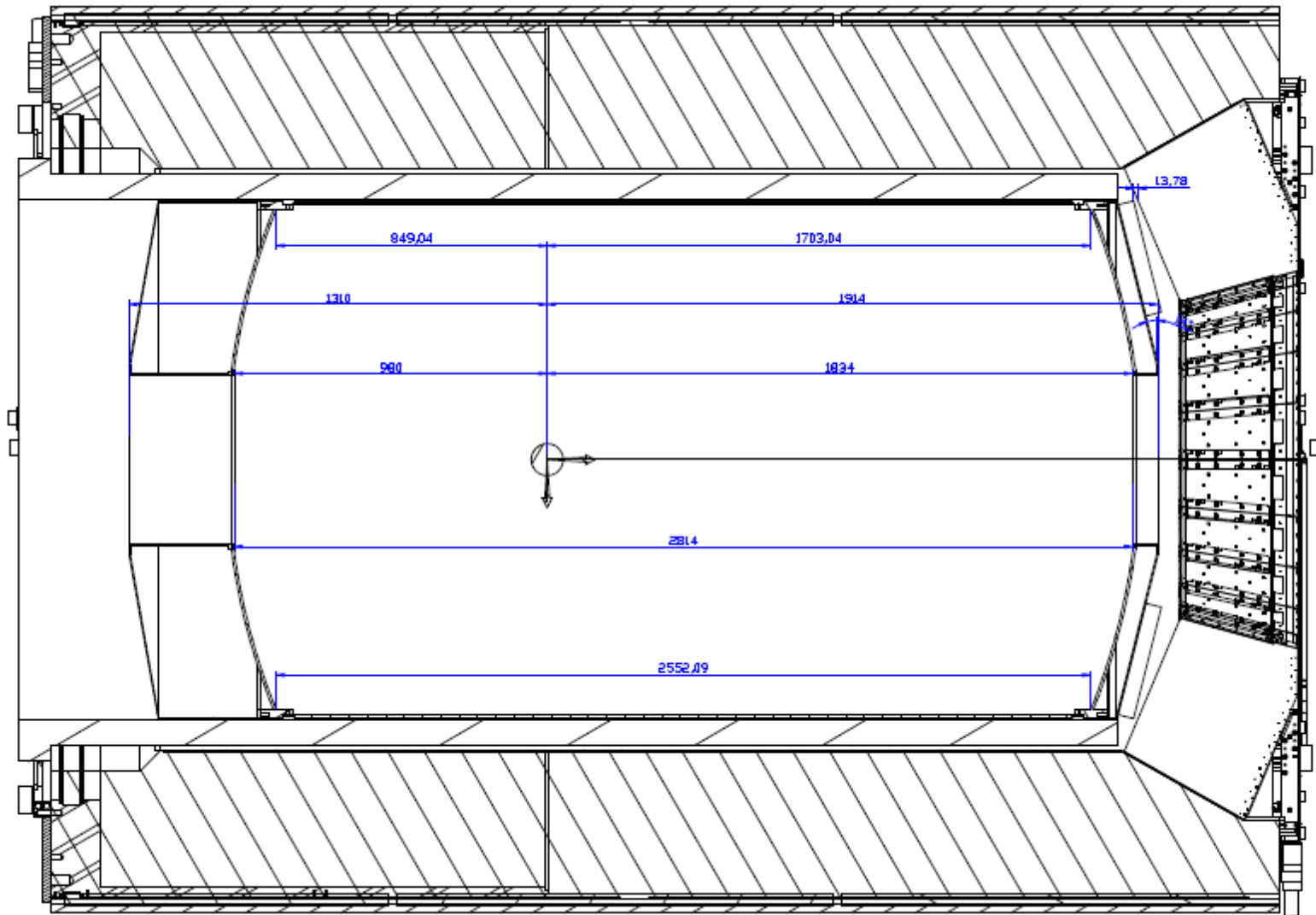
Drawing from Stefano Lauciani, LNF

4) CONCAVE dimensions -1310 +1793



Drawing from Stefano Lauciani, LNF

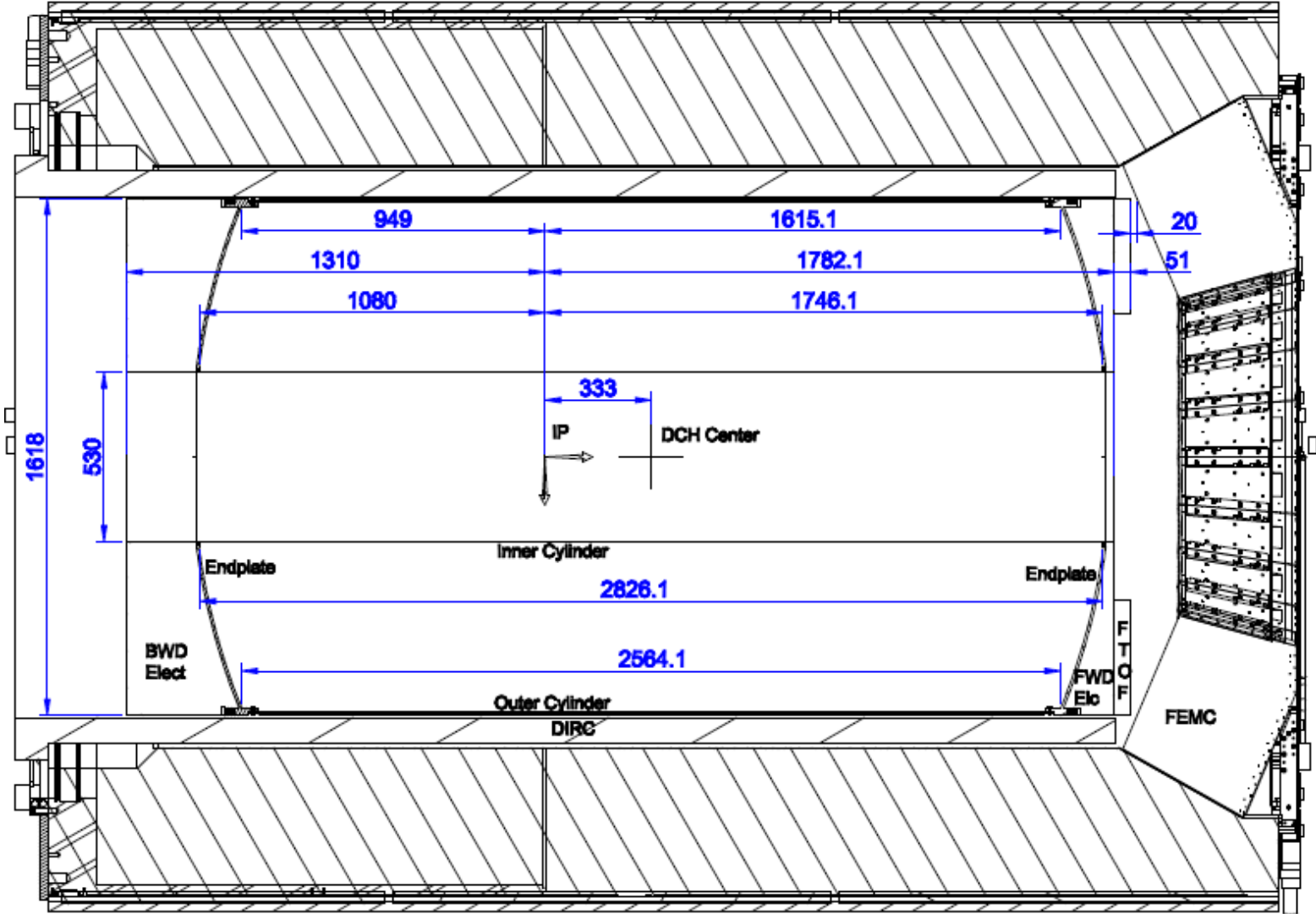
5) CONVEX dimensions -1310 +1914



210 mm

Drawing from Stefano Lauciani, LNF

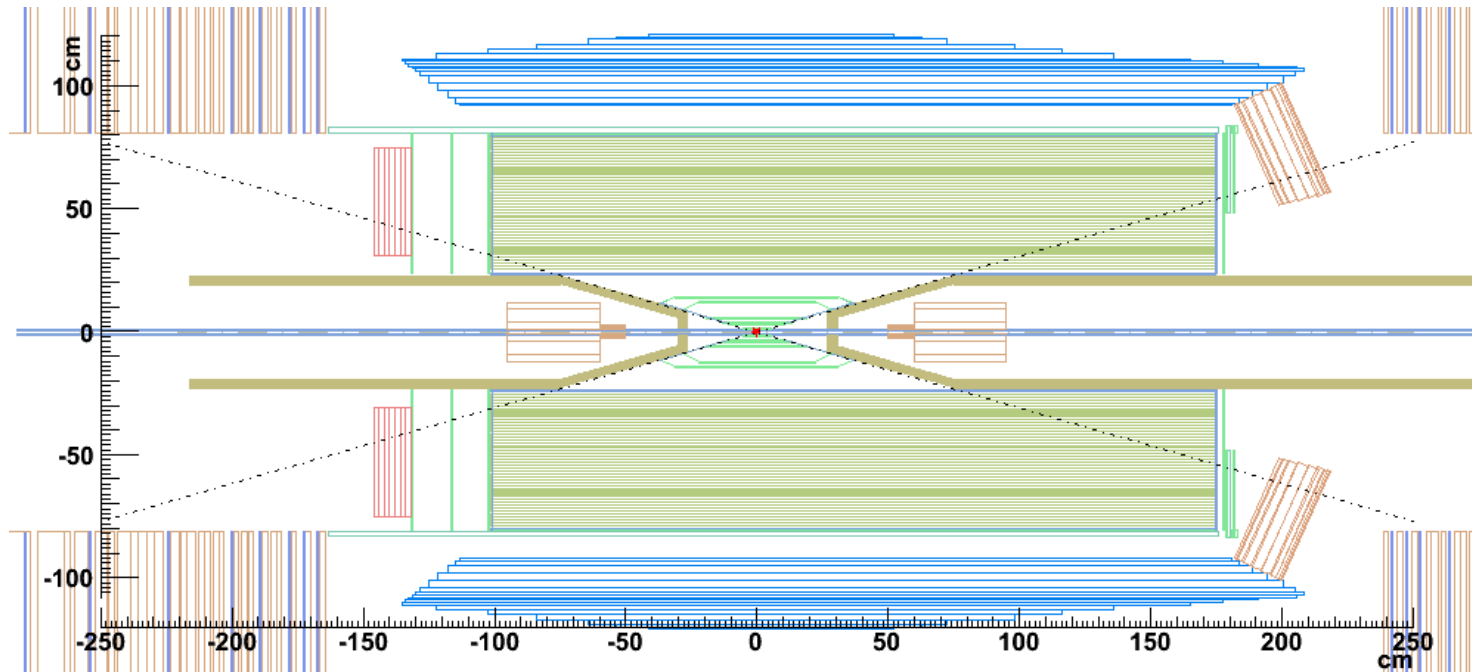
Option 7



Drawing from Stefano Lauciani, LNF

Option 6

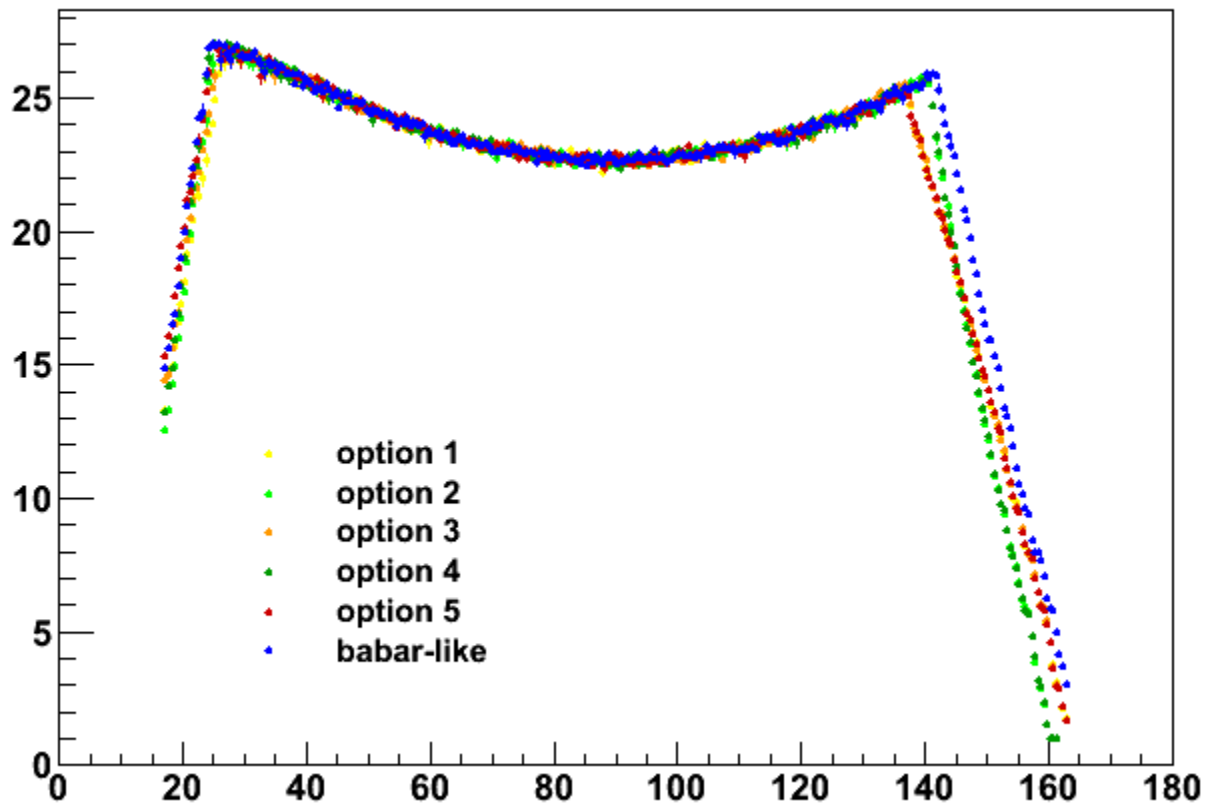
x-z layout in fastsim



old SuperB (babar-like) configuration

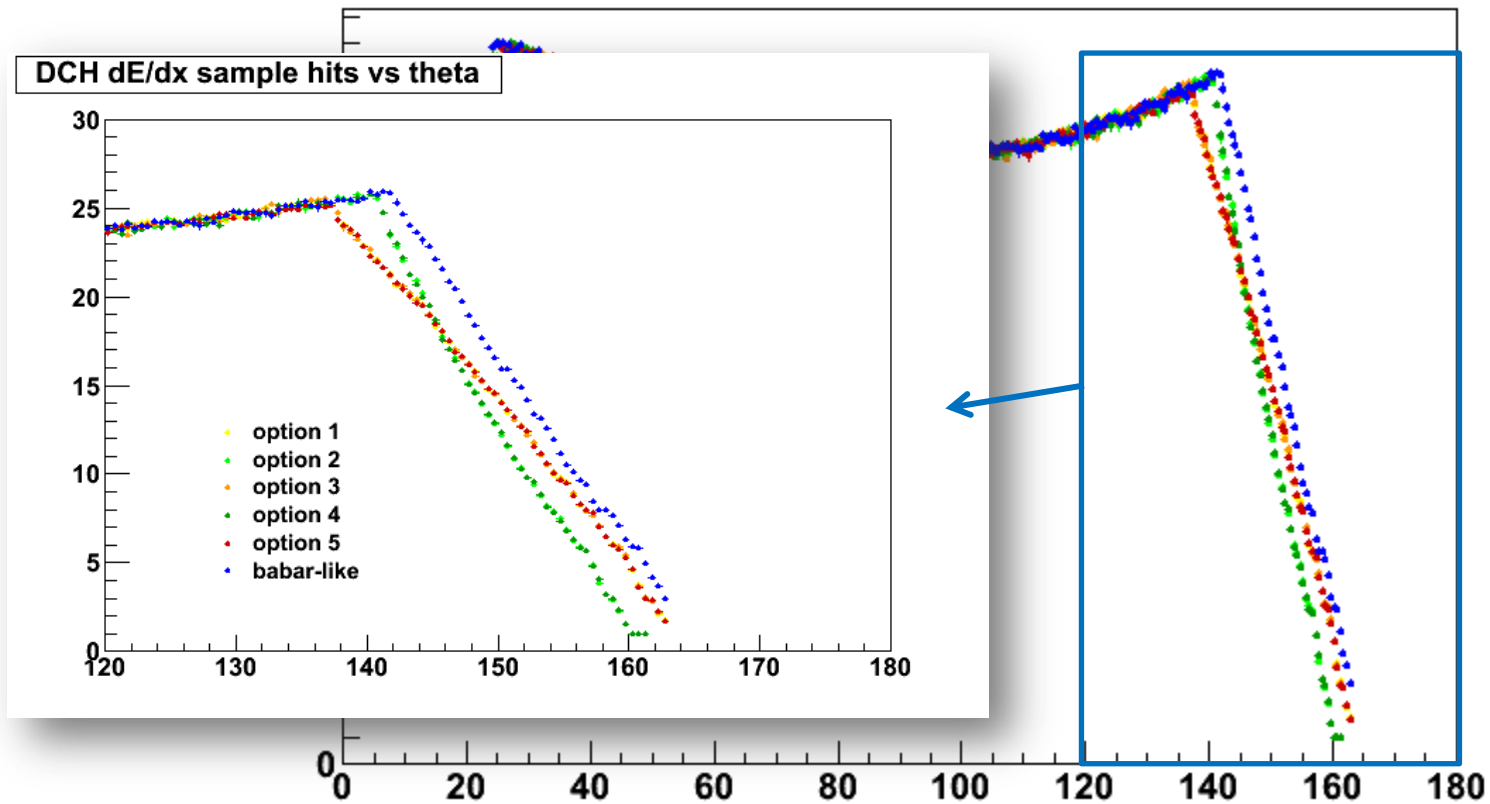
single π^+ , $p=4\text{GeV}/c$, flat $\cos\theta$

DCH dE/dx sample hits vs theta



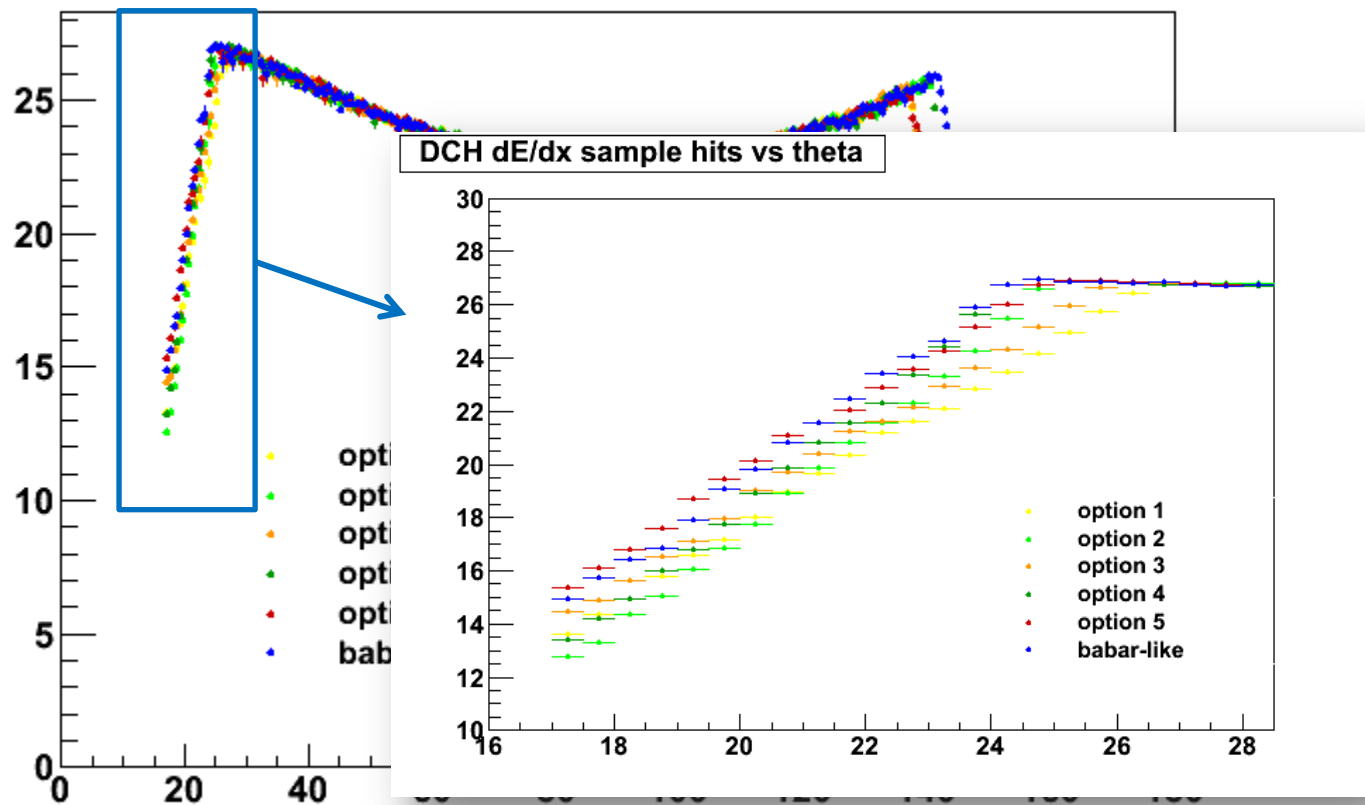
single π^+ , $p=4\text{GeV}/c$, flat $\cos\theta$

DCH dE/dx sample hits vs theta



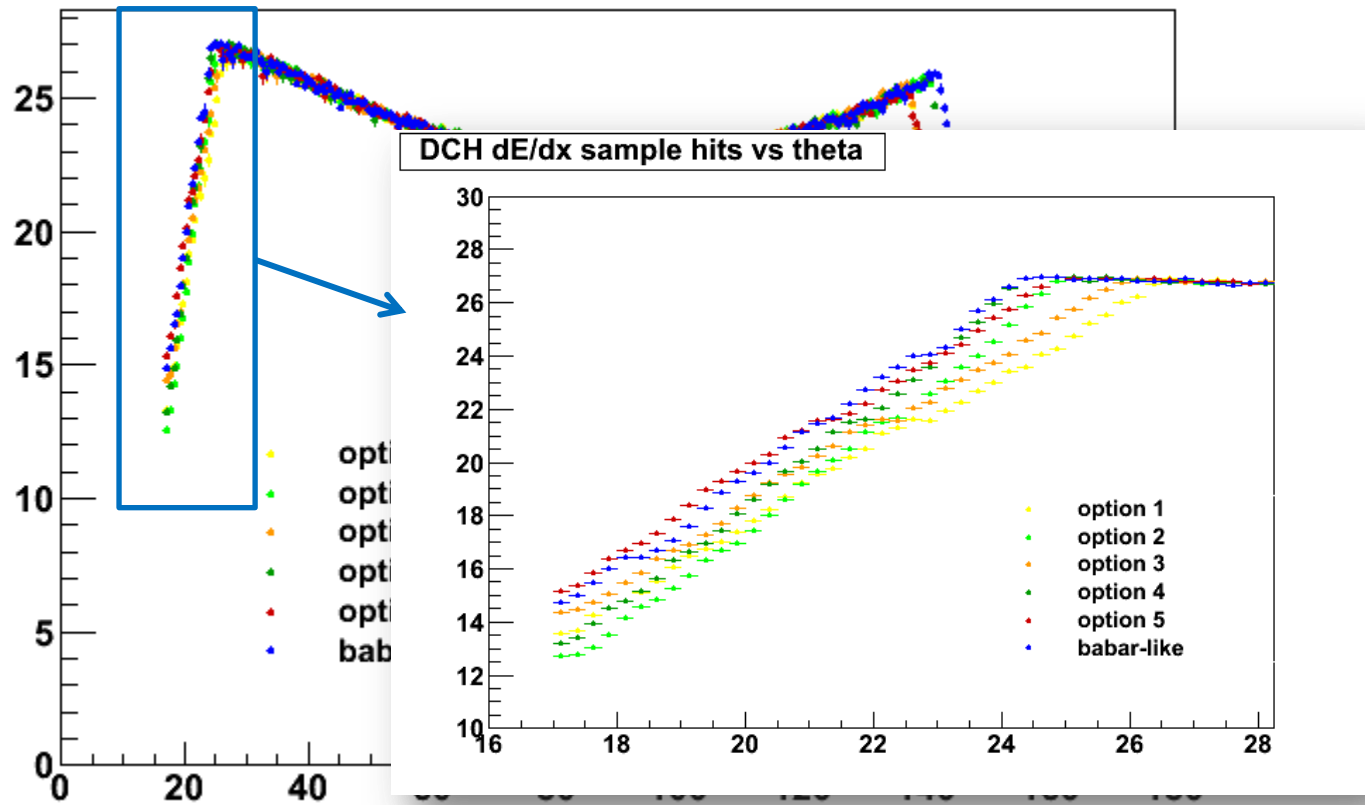
single π^+ , $p=4\text{GeV}/c$, flat $\cos\theta$

DCH dE/dx sample hits vs theta

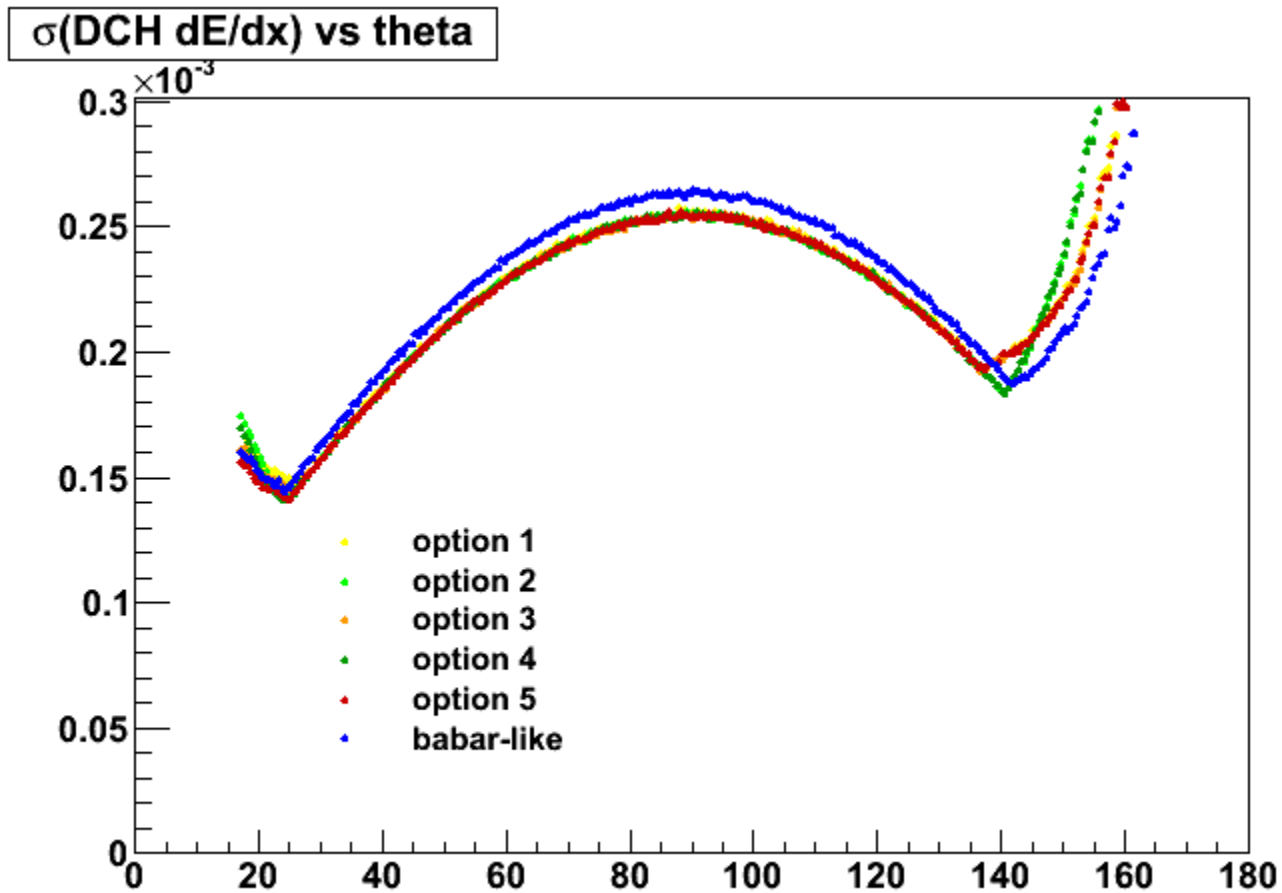


single π^+ , $p=4\text{GeV}/c$, flat $\cos\theta$

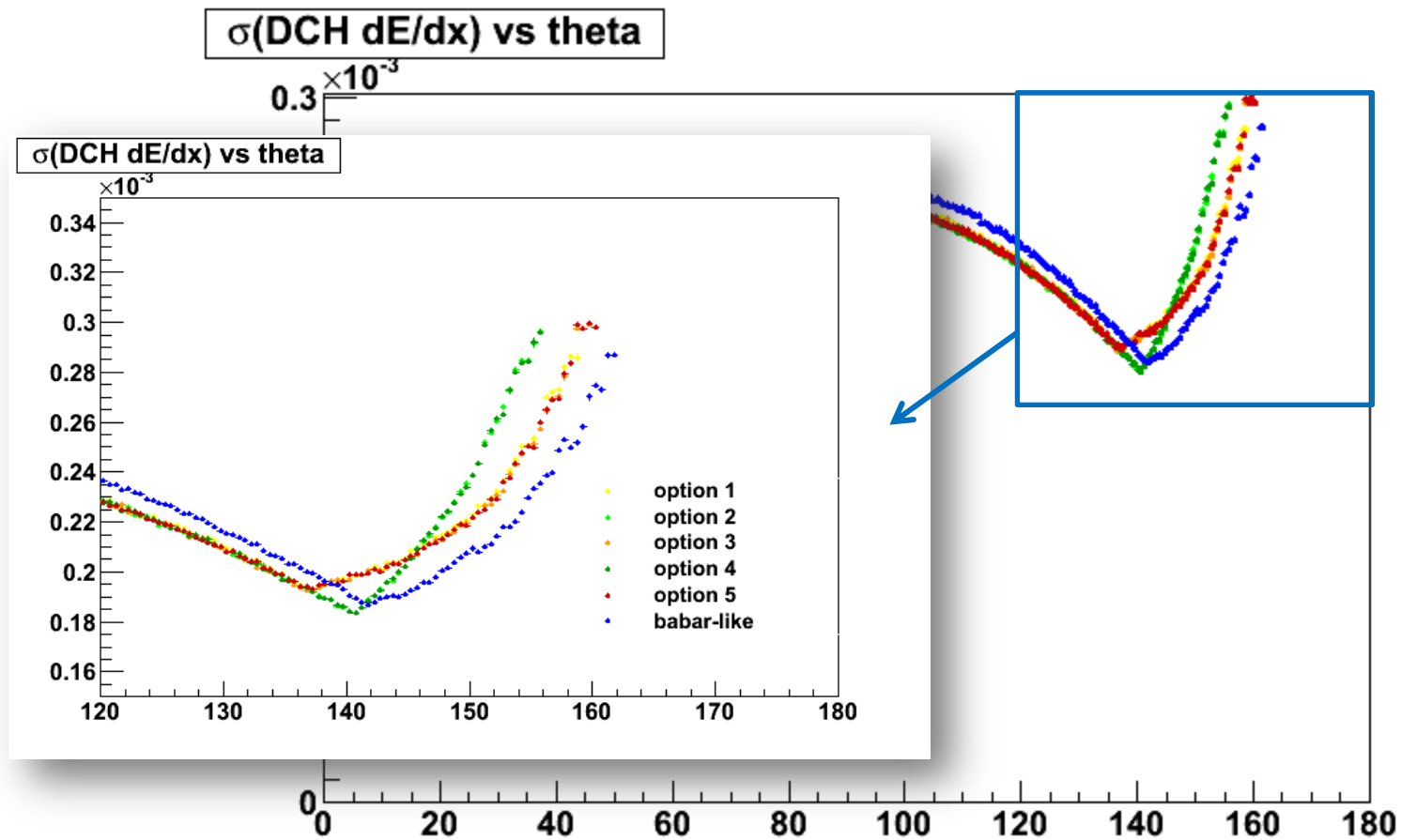
DCH dE/dx sample hits vs theta



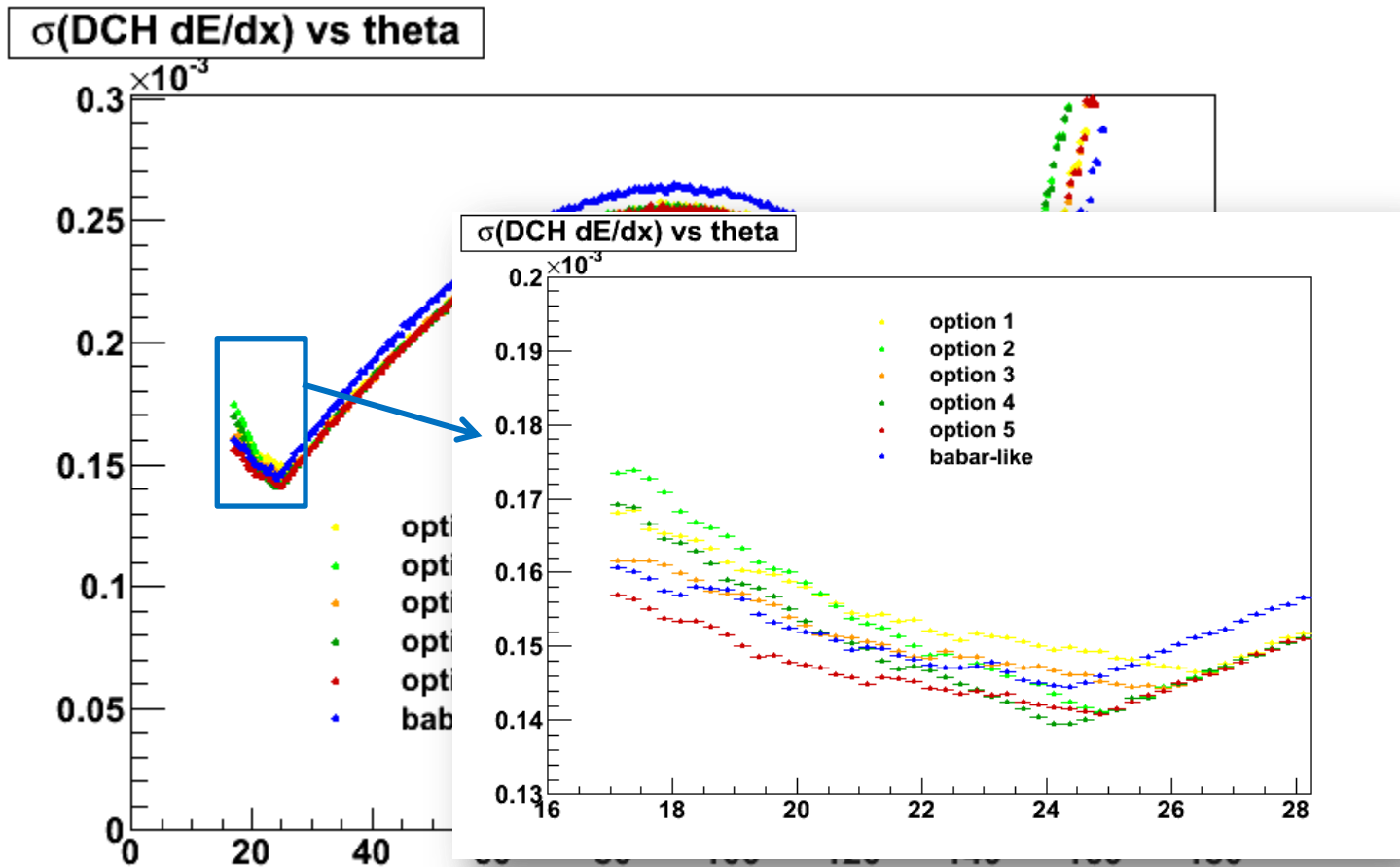
single π^+ , $p=4\text{GeV}/c$, flat $\cos\theta$



single π^+ , $p=4\text{GeV}/c$, flat $\cos\theta$

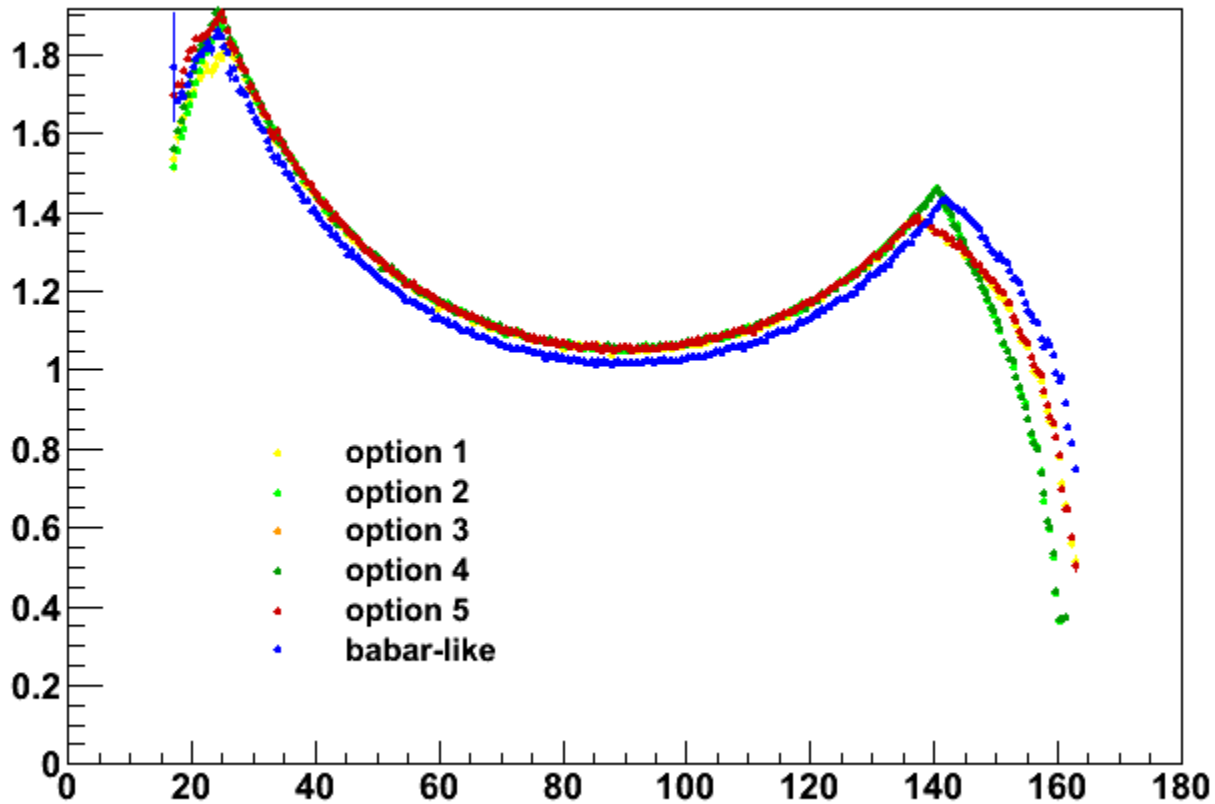


single π^+ , $p=4\text{GeV}/c$, flat $\cos\theta$



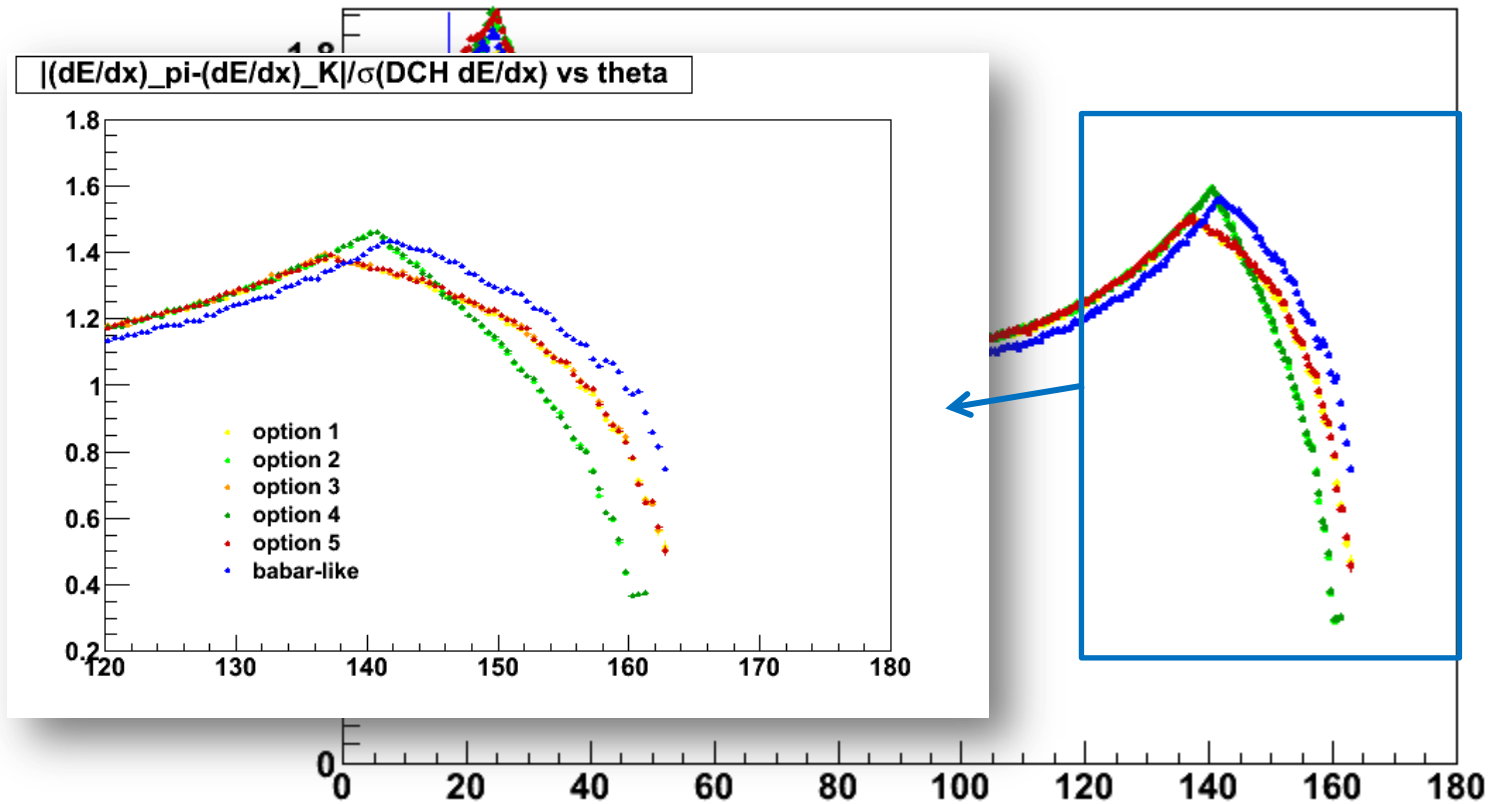
single π^+ , $p=4\text{GeV}/c$, flat $\cos\theta$

$|(dE/dx)_{\pi} - (dE/dx)_K| / \sigma(\text{DCH } dE/dx)$ vs theta



single π^+ , $p=4\text{GeV}/c$, flat $\cos\theta$

$|(\text{dE/dx})_{\text{pi}} - (\text{dE/dx})_{\text{K}}| / \sigma(\text{DCH dE/dx})$ vs theta



single π^+ , $p=4\text{GeV}/c$, flat $\cos\theta$

$|(dE/dx)_{\pi} - (dE/dx)_K| / \sigma(\text{DCH } dE/dx)$ vs theta

